
Towards Practical Multi-label Causal Discovery in High-Dimensional Event Sequences via One-Shot Graph Aggregation

Hugo Math^{1,2} Rainer Lienhart²

¹ BMW Group

² Chair for Machine Learning and Computer Vision, Augsburg University
Augsburg, Germany
hugo.math@bmwgroup.de, rainer.lienhart@uni-augsburg.de

Abstract

Understanding causality in event sequences where outcome labels such as diseases or system failures arise from preceding events like symptoms or error codes is critical—yet remains an unsolved challenge across domains like healthcare or vehicle diagnostics. We introduce CARGO, a scalable multi-label causal discovery method for sparse, high-dimensional event sequences consisting of thousands of unique event types. Using two pretrained causal Transformers as domain-specific foundation models for event sequences—CARGO infers in parallel, per sequence, one-shot causal graphs and aggregates them using an adaptive frequency fusion to reconstruct the global Markov boundaries of labels. This two-stage approach enables efficient probabilistic reasoning at scale while avoiding the intractable cost of full-dataset conditional-independence testing. Our results on a challenging real-world automotive fault prediction dataset with over 29,100 unique event types and 474 imbalanced labels demonstrate CARGO’s ability to perform structured reasoning.

1 Introduction

Understanding *why* specific events lead to particular outcomes is vital for effective diagnosis, predictions, and overall decision-making [24, 36]. For instance, “what series of events captured by diagnostic led to this vehicle failure” or “what symptoms led to this disease” [27, 39, 15, 25, 34]. Here, an event sequence consists of a list of discrete events x_i recorded asynchronously over time, while labels y summarize outcomes associated with the full sequence (e.g, a diagnosed defect or condition).

A fundamental obstacle in these settings is dimensionality. Real-world systems often involve tens of thousands of possible events, rendering causal discovery intractable for current algorithms [14]. To address this, we reinterpret multi-label causal discovery for event sequences as a form of Bayesian model averaging [16, 33], where each sequence is treated as a sample from a local causal model. Specifically, each sequence induces a one-shot causal graph (i.e., a directed acyclic graph (DAG)) [40]. Together, they can be fused to form a unified global structure [6]. This process, known as structural fusion [32], aggregates local graphs into a consensus causal graph over all observed sequences.

To summarize our contributions: we introduce CARGO (Causal Aggregation via Regressive Graph Operations), the first method to provide scalable causal discovery across thousands of labelled event sequences, with theoretical guarantees under standard assumptions. It is divided into two phases: (1)

One-shot graph extraction, where for each sequence, CARGO infers the local Markov boundary of each label using two autoregressive Transformers as density estimators [48, 10] (2) Graph fusion, where the local graphs are aggregated via an adaptive threshold function to provide global Markov Boundaries.

We empirically validate CARGO on a large-scale vehicular dataset comprising about 29,100 events and 474 imbalanced labels, demonstrating, for the first time, scalability and practical superiority over traditional causal discovery baselines. We also perform ablation on scoring criteria, frequency thresholds, and Transformer quality.

2 Preliminary & Related Work

A full description of the notations and definitions used throughout the paper can be found in Appendix A.

Event Sequence Modelling. Event sequences are typically represented as a series of time-stamped discrete events $S = \{(t_1, x_1), \dots, (t_L, x_L)\}$ where $0 \leq t_1 < \dots \leq t_L$ denotes the time of occurrence of event type $x_i \in \mathbb{X}$ drawn from a finite vocabulary \mathbb{X} . In multi-label settings, a binary label vector $\mathbf{y} \in \{0, 1\}^{|\mathbb{Y}|}$ is attached to S and indicates the presence of multiple outcome labels chosen from \mathbb{Y} occurring at the final time step t_L . Together, this results in a multi-labeled sequence $S_l = (S, (\mathbf{y}_L, t_L))$.

Event sequence modelling has been widely applied to predictive tasks. For instance, in the automotive domain, Diagnostic Trouble Codes (DTCs) [34] are logged asynchronously over time and used to infer failures or error patterns [28]. In healthcare, electronic health records encode temporal sequences of symptoms to perform predictive tasks [39, 20, 15]. A common modelling strategy [22, 29] separates such event types \mathbb{X} from labels \mathbb{Y} .

Transformers [48, 38, 45] have emerged as the dominant architecture for sequence modelling. Recent work leveraged Transformers in high-dimensional event spaces for next-event and label prediction. Math et al. [28] proposed a dual Transformer architecture in which one model predicts the next event type (DTC) and the other predicts label occurrence (e.g., error patterns). Through this paper, we repurpose this dual architecture for causal discovery.

Multi-label Causal Discovery seeks to identify the Markov Boundary (**MB**) of each label—its minimal set of parents, children, and spouses—such that the label is conditionally independent of all other variables given its **MB** [46] (Def. 3).

While classical constraint-based algorithms have shown success on low-dimensional tabular data [41, 52], their application to event sequences with multi-label outputs remains challenging due to: (1) *dimensionality*—thousands of event types increase super-exponentially the number of graphs (2) *sparsity*—multi-hot encodings often underrepresent rare but important events (3) *distributional assumptions*—such as linearity or Gaussian noise, which rarely hold in real-world sequences [12].

Contemporary work points to decomposing classical causal discovery for high-dimensional datasets into sub-problems and graph aggregation. Laborda et al. [21] introduce a ring-based distributed algorithm for learning high-dimensional BN, Dong et al. [6] explores a distributed approach for large-scale causal structure learning and Mokhtarian et al. [30] for Markov Boundaries.

Bayesian Network [33] has served as a modelling technique for a variety of decision problems. It is defined as a triplet $\langle \mathbf{U}, \mathbb{G}, P \rangle$ with P the joint distribution over a variable set \mathbf{U} of a directed acyclic graph $\mathbb{G} = (\mathbf{U}, E)$ with E as the set of directed edges. This triplet must satisfy the Markov Condition: every random variable U_i is independent of its non-descendant variables given its parents $\text{Pa}(U_i)$ in \mathbb{G} . The directed edge $(U_i \rightarrow U_j)$ encodes a probabilistic dependence. Thus, the joint probability distribution can be factorized as:

$$P(U_1, \dots, U_n) = \prod_{i=1}^n P(U_i | \text{Pa}(U_i))$$

The DAG encodes a set of conditional independencies $\mathcal{I}(\mathbb{G})$, where each element corresponds to a conditional independence relation $U_i \perp U_j | \mathbf{Z}$, meaning that U_i and U_j are conditionally independent

given the set of variables Z . Formally, a DAG \mathbb{G}_k is an I-map (or Independence map) of another \mathbb{G} if the set of conditional independencies encoded by \mathbb{G}_k is a subset of those encoded by \mathbb{G} :

$$\mathcal{I}(\mathbb{G}_k) \subseteq \mathcal{I}(\mathbb{G})$$

\mathbb{G}_k is a minimal I-map of \mathbb{G} if removing any edge from it introduces a conditional dependence that would violate an independence in \mathbb{G} , i.e. $\mathcal{I}(\mathbb{G}_k \setminus \{e\}) \not\subseteq \mathcal{I}(\mathbb{G}) \forall e \in E$.

Bayesian Model Averaging. Fusing BN has several direct applications. Either to average multiple models from different experts to learn a global and average representation [16]. Or to perform causal discovery in distributed settings with federated learning algorithms [50, 13].

Formally, Given a set of Bayesian Networks $\{B_k\}_{k=1}^m$ with associated DAGs $\{\mathbb{G}_k = (V_k, E_k)\}_{k=1}^m, V_k \in \mathbf{U}$ sharing the same finite set of node \mathbf{U} , structural fusion aim to construct the DAG $\mathbb{G}^* = (V, E), V \in \mathbf{U}$. Multiple fusion methods exist and leverage either the probability distribution p by doing Bayesian Model Averaging [16] or focus on the structural learning (Fig. 8) of \mathbb{G}^* [5, 32, 11, 35, 13], which is an NP-hard [32] problem.

We will focus on the second element in this paper. Hence, we are seeking the merged edges $E = \bigcup_{i=1}^m E_i^\sigma$. The consistent node ordering σ ensures acyclicity. The fused DAG \mathbb{G}^* is the minimal I-map of the intersection of the conditional independencies across all DAGs $\mathbb{G}_k = (V_k, E_k)\}_{k=1}^m$.

Greedy Equivalence Search. (GES) [2] is one of the most theoretically sound methods to recover a Markov equivalence class (MEC, Def. 4) of a DAG. In large-sample settings, GES provides theoretical guarantees of recovering the true graph. Formally, GES searches for the MEC of the graph \mathbb{G}^* from the observational dataset D with distribution p . This defines the optimization problem as:

$$\mathbb{G}^* = \arg_{\mathbb{G}} \max S(\mathbb{G}, D) \quad (1)$$

Chickering [2] proved that under parametric assumption, a large number of samples and using the Bayesian Information Criterion (BIC) as criterion S , GES is guaranteed to recover a Markov Equivalence Class of \mathbb{G}^* .

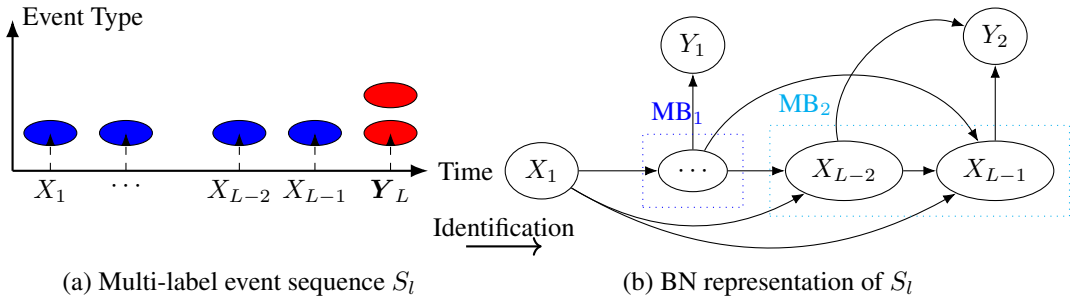
Frequency Based. Multiple heuristics have been developed to merge multiple BNs. One is edge frequency cutoff [43], other on estimating the proportion of false positive edges [8] and integer linear programming (ILP) [8] or a mix of both: [44]. As pointed out by [8], choosing a frequency cutoff τ is particularly challenging. Moreover, under class imbalance and long-tail problem in classification [53], the theoretical property of frequency approaches, such as the law of large numbers, might not hold.

We will now explain the two phases of CARGO, which are (1) One-shot causal discovery (2) Graph aggregation using adaptive thresholds. The Proofs of Lemmas and Theorems can be found in the Appendix B.

3 One-Shot Causal Discovery

Let S_l^k be a multi-labeled sequence drawn from a dataset $D = \{S_l^1, \dots, S_l^m\} \subset \mathbb{S}$ and \mathbb{G}_k the sequential BN (Fig. 1) with attached labels. The goal of multi-label causal discovery is to identify the

Figure 1: An example of a causal graph extracted from a single multi-label **event** sequence where **MB₁** represents the Markov Boundary of Y_1 and **MB₂** the Markov Boundary of Y_2 .



Markov Boundary of each label $Y_j \in \mathbf{Y}$ present in S_l^k . To be able to access conditional independence (Def. 2) between X_i and Y_j conditioned on the past events $\mathbf{Z} = (x_1, \dots, x_{i-1}) = S_{<i}$, we model the event apparitions using a sequential BN (Fig. 1).

We want to assess how much additional information event X_i occurring at step i provides about label Y_j when we already know the past sequence of events $\mathbf{Z} = S_{<i}$. We essentially try to answer if:

$$P(Y_j|X_i, \mathbf{Z}) = P(Y_j|\mathbf{Z}) \Leftrightarrow D_{KL}(P(Y_j|X_i, \mathbf{Z})\|P(Y_j|\mathbf{Z})) = 0$$

where D_{KL} denotes the *Kullback-Leibler divergence* [3]. The distributional difference between the conditionals $P(Y_j|X_i, \mathbf{Z}), P(Y_j|\mathbf{Z})$ is akin to Information Gain I_G [37] conditioned on past events:

$$I_G(Y_j, x_i|z) \triangleq D_{KL}(P(Y_j|X_i = x_i, \mathbf{Z} = z)\|P(Y_j|\mathbf{Z} = z)) \quad (2)$$

Which is equals to the difference between the conditional entropies [3] denoted as H :

$$I_G(Y_j, x_i|z) = H(Y_j|z) - H(Y_j|x_i, z) \quad (3)$$

More generally, we can access the conditional independence of event X_i and label Y_j using the conditional mutual information (CMI) [3] which is simply the expected value over z of the information gain $I_G(Y_j, X_i|z)$ such as:

$$I(Y_j, X_i|\mathbf{Z}) \triangleq H(Y_j|\mathbf{Z}) - H(Y_j|\mathbf{Z}, X_i) = \mathbb{E}_{p(z)}[I_G(Y_j, X_i|\mathbf{Z} = z)] \quad (4)$$

It can be interpreted as the expected value over all possible contexts \mathbf{Z} of the deviation from independence of X_i, Y_j in this context. To approximate Eq. (4), a naive Monte Carlo [7] approximation is performed where we draw N random variations of the conditioning set $z^{(l)} = \{x_0^{(l)}, \dots, x_{i-1}^{(l)}\}$, denoting the l -th sampled particle:

$$\hat{I}_N(Y_j, X_i | \mathbf{Z}) = \frac{1}{N} \sum_{l=1}^N I_G(Y_j, X_i | \mathbf{Z} = z^{(l)}) \quad (5)$$

This estimator is unbiased because the contexts $z^{(l)}$ are sampled directly from Tf_x using a proposal Q with the same support as $P(\mathbf{Z})$. Since $I_G(Y_j, X_i | \mathbf{Z} = z)$ is a difference between conditional entropies ((2)), it is thus bounded uniformly [3] by the log of supports such as:

$$0 < I_G(Y_j, X_i | \mathbf{Z} = z^{(l)}) = H(Y_j|z^{(l)}) - H(Y_j|X_i, z^{(l)}) \leq H(Y_j) \leq \log |\mathbb{Y}|$$

Thus the posterior variance of $f_i = I_G(Y_j, X_i | \mathbf{Z} = z^{(l)})$ satisfies $\sigma_{f_i}^2 \triangleq \mathbb{E}_{p(z)}[f_i^2(p(z)) - I^2(f_i)] < +\infty$ [7] then the variance of $\hat{I}_N(f_i)$ is equal to $\text{var}(\hat{I}_N(f_i)) = \frac{\sigma_{f_i}^2}{N}$ and from the strong law of large numbers:

$$\hat{I}_N \xrightarrow[N \rightarrow +\infty]{\text{a.s.}} \mathbb{E}_{p(z)}[I_G(Y_j, X_i | \mathbf{Z} = z)] \triangleq I(f_i). \quad (6)$$

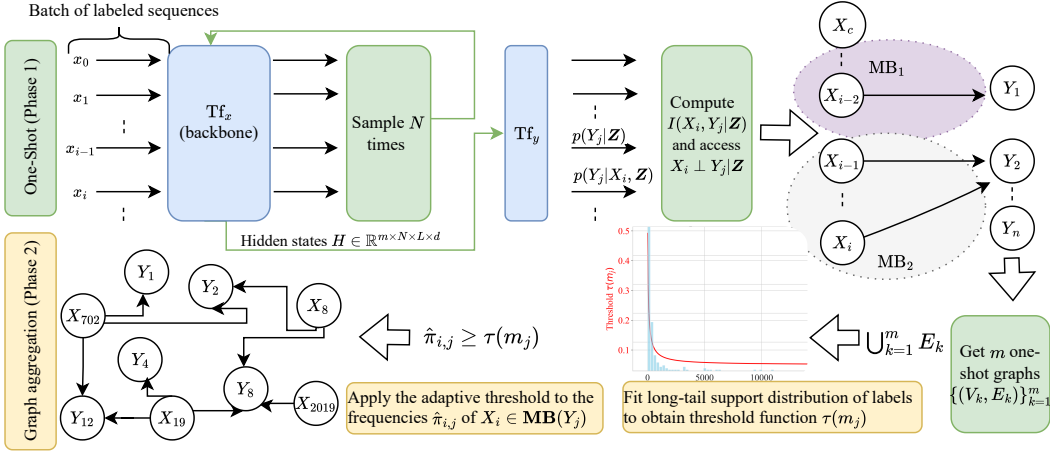
Density Estimation. We used two pretrained Transformers (Tf_x, Tf_y) trained via maximum likelihood on a dataset of multi-labelled event sequences $D = \{S_l^1, \dots, S_l^m\} \subset \mathbb{S}$. We assume that they perfectly model the true conditional distributions of events and labels (A4). While, due to the strict equivalences between CI-tests and conditional independence, it is difficult to provide a theoretical guarantee under imperfect models, we acknowledge that this assumption may be violated. We note that most causal discovery methods either impose strong parametric data assumptions or rely on a perfect CI-test. We provide an ablation study on the impact of the NADE's quality on the one-shot phase in Appendix C.1, including the number of parameters, context c , and Tf_y performance.

Formally, the two Transformers infer the probability of the next event and label conditioned on the past events using the hidden states $\mathbf{h}_{i-1}^x, \mathbf{h}_i^y \in \mathbb{R}^d$, from Tf_x, Tf_y respectively:

$$\text{Tf}_x(S_{<i}) = \text{Softmax}(\mathbf{h}_{i-1}^x) = P_{\theta_x}(X_i|\mathbf{Z}) \quad (7)$$

$$\text{Tf}_y(S_{\leq i}) = \text{Sigmoid}(\mathbf{h}_i^y) = P_{\theta_y}(Y|X_i, \mathbf{Z}) \quad (8)$$

Figure 2: The overview of CARGO. Phase 1 (One-shot) is on top, and Phase 2 (Adaptive Thresholding) is on the bottom. d denotes the hidden dimension, L the sequence length, m the number of samples and MB_1, MB_2 the Markov Boundary of Y_1, Y_2 . All green and blue areas are parallelized.



Sequential One-shot Causal Discovery. The CMI using Eq.(4) is computable only with the posteriors $P(Y_j|Z)$, $P(Y_j|X_i, Z)$. In practice a label-specific threshold $\theta_j \approx 0$ is applied to Eq. (4) to identify conditional dependence:

$$Y_j \not\perp X_i \mid Z \Leftrightarrow I(Y_j, X_i \mid Z) > \theta_j \approx 0. \quad (9)$$

Hence, the expectation in Eq.(4) is computed using a Monte-Carlo simulation, by sampling N similar context Z from Tf_x . Such that for each position in the sequence, we generate N plausible next tokens using a combination of top-k and nucleus sampling [17]. Ablation studies on the effect of the sampling method and thresholds are given in Appendix C.2, C.3.

Theorem 1 (Markov Boundary Identification in Event Sequences). *If S_l^k a multi-labeled sequence drawn from a dataset $D = \{S_l^1, \dots, S_l^m\} \subset \mathbb{S}$ where two Oracle Models Tf_x and Tf_y were trained on, then under causal sufficiency (A3), bounded lagged effects (A2) and temporal precedence (A1), the Markov Boundary of each label Y_j in the causal graph \mathbb{G} can be identified using conditional mutual information for CI-testing.*

Theorem 1 enables us to sequentially recover the Markov Boundary of each label in a sequence. It provides a theoretical guarantee to recover the correct causes for each label Y_j .

Computation. A key advantage of our approach is its scalability. Unlike traditional methods whose complexity depends on the event and label cardinality $|\mathbb{X}|$ and $|\mathbb{Y}|$ [23], phase 1 is agnostic to both. Figure 2 shows all parallelized steps on GPUs. CMI estimations are independently performed for all positions $i \in [c, L]$, with the sampling pushed into the batch dimension and results averaged across labels. This transitions the time complexity from $\mathcal{O}(\text{BS} \times N \times L)$ to $\mathcal{O}(1)$ per batch, with L being the sequence length.

To ensure stable conditional entropy estimates and reliable predictions from Tf_y , the CMI is computed after observing c events (*context*). This design choice also enables out-of-the-box parallelization. By sampling N variations of the prefix sequence $S_{\leq c}$, the CMI is independently computed across positions $i \in [c, L]$. In our experiments, we set $c = 15$, $L = 192$. The implementation of Phase 1 in PyTorch [31] is provided in Appendix D.2.

4 Structural Fusion of Markov Boundaries

Let $\{\mathbb{G}_k = (V_k, E_k)\}_{k=1}^m, V_i \in \mathbf{U}$ be the set of DAGs generated by the Phase 1 from the dataset D containing m i.i.d sequences $\{S_l^k\}_{k=1}^m$ drawn from a joint distribution $p(x, y)$. Each graph \mathbb{G}_k represents local Markov Boundaries identified within sequence S_l^k . Our objective is to fuse these

local graphs into a single, global consensus graph $\mathbb{G}^* = (\mathbf{U}, \mathbf{E})$ (see Fig. 8) with the events always as parents of labels Y_j such as:

$$\text{Pa}(Y_j) \subseteq \{X_1, \dots, X_n\}$$

A naive fusion approach, such as taking the simple union of all edges $E = \bigcup_{k=1}^m E_k^\sigma$ works iff the Oracle models yield the perfect CI-tests in Phase 1 and thus the local graphs \mathbb{G}_k^k are faithful to $p(x, y)$ ([32], Theorem 4.). Here, the ordering σ doesn't matter since we are dealing with Markov Boundaries. Moreover, G^* is naturally a DAG because we considered previously that outcome labels are solely explained by events, which simplifies acyclicity. We define the Bernoulli variable $Z_{i,j}^k$ for each potential edge $(X_i \rightarrow Y_j)$ within each sequence S_i^k :

$$Z_{i,j}^k = \begin{cases} 1 & \text{if the edge } X_i \rightarrow Y_j \text{ is present in } \mathbb{G}_k \\ 0 & \text{otherwise} \end{cases}$$

Under the Oracle Models assumption (A4), our one-shot discovery phase serves as a perfect conditional-independence tester. Consequently, the detection of an edge in a local graph \mathbb{G}_k corresponds precisely to a true causal dependency in the global graph \mathbb{G}^* . The probability of this event $P(Z_{i,j}^k = 1)$ is therefore the true marginal probability of the edge's existence, which we denote as $\pi_{i,j}$.

The empirical frequency, $\hat{\pi}_{i,j}(m)$, of the edge $(X_i \rightarrow Y_j)$ after observing m sequences is the sample mean of these i.i.d Bernoulli variables $\hat{\pi}_{i,j}(m) = \frac{1}{m} \sum_{k=1}^m Z_{i,j}^k$. By the Law of Large Numbers (LLN), as the number of i.i.d sequences m tends to infinity, the empirical frequency converges in probability to the true expected value of the random variable:

$$\hat{\pi}_{i,j}(m) \xrightarrow{P} \mathbb{E}[Z_{i,j}^k] = \pi_{i,j}$$

Thus, given a sufficiently large number of sequences, the empirical frequency $\hat{\pi}_{i,j}(m)$ serves as a consistent estimator for the true probability of the edge's existence in the global DAG \mathbb{G}^* .

4.1 Aggregation under imperfect CI-tests

The assumption of an Oracle CI-tester, while necessary for initial theoretical guarantees, is invariably violated in practice due to factors like model capacity, limited data, or class imbalance. The extracted one-shot graphs will most likely violate the independencies in \mathbb{G}_k and thus \mathbb{G}^* .

Let us model the performance of our one-shot CI-test for any potential edge $X_i \rightarrow Y_j$ with the following error rates: (1) False Positive Rate (Type I Error): $\alpha = P(\text{detect} \mid \text{edge is spurious})$ (2) True Positive Rate (Sensitivity): $1 - \beta = P(\text{detect} \mid \text{edge is causal})$. We operate under the reasonable assumption that our one-shot classifier is significantly better than random, which implies that $1 - \beta \gg \alpha$. The expected value of our Bernoulli variable $Z_{i,j}^k$ is now:

$$\begin{aligned} \mathbb{E}[Z_{i,j}^k] &= P(Z_{i,j}^k = 1) \\ &= P(\text{detect} \mid \text{causal})P(\text{causal}) + P(\text{detect} \mid \text{spurious})P(\text{spurious}) \\ &= (1 - \beta)\pi_{i,j} + \alpha(1 - \pi_{i,j}) \end{aligned}$$

The empirical frequency now converges to this new expectation. For a true edge ($\pi_{i,j} = 1$), the empirical frequency converges to a high value: $\hat{\pi}_{i,j}(m) \xrightarrow{P} 1 - \beta$ and for a spurious edge ($\pi_{i,j} = 0$) it converges to a low value: $\hat{\pi}_{i,j}(m) \xrightarrow{P} \alpha$. This reveals the critical role of frequency aggregation as a mechanism for separating signal from noise.

4.2 Adaptive Fusion for Structural Discovery in Long-Tail Distributions

A primary challenge in real-world causal discovery is the long-tail distribution of outcome labels, where a few “head” labels possess abundant data while the vast majority of “tail” labels are data-sparse [53].

For rare labels, where empirical edge frequencies are high-variance estimators, a conservative high threshold is necessary to maintain precision against statistical noise. Conversely, for common labels where frequencies are reliable, a high threshold would be overly stringent, purging weaker but valid

Figure 3: Example of an error pattern (y_1) defined as a boolean rules of diagnosis trouble codes (x_i)

$$y_1 = x_1 \& x_5 \& x_8 \& x_{18} \& x_{12} \& x_3 \& !x_{10} \& !x_{20}$$

causal links. To resolve this, we introduce an adaptive thresholding strategy (Fig. 7) that tailors the edge inclusion criterion to the statistical power available for each label. We define a label-specific threshold τ_j , as a logistic decay function of its sample support m_j :

$$\tau_j(m_j) = (\tau_{\max} - \tau_{\min}) \cdot \frac{1}{1 + e^{k(\log m_j - \log m_0)}} + \tau_{\min} \quad (10)$$

This function smoothly interpolates between a user-defined maximum threshold, τ_{\max} (prioritizing precision for the tail), and a minimum, τ_{\min} (prioritizing recall for the head). Crucially, the function’s behavior is calibrated by the distribution of the data. Such that decay midpoint m_0 is set to the median of all label supports, providing a robust anchor point against skew.

The decay rate, k is made inversely proportional to the log-inter-quartile range of supports such that $k = \frac{2 \log 3}{\log q_{75} - \log q_{25}}$. For rare labels with small m_j , the high variance of the frequency estimate necessitates a high threshold $\tau_j(m_j)$ that acts as a strong regularizer. For common labels with large m_j , the LLN guarantees the convergence of $\hat{\pi}_{i,j}$ to the true edge probability, justifying a lower threshold to capture a more complete causal structure. Hence, this strategy serves as a data-driven denoising mechanism and shares theoretical parallels with ensembling methods [1, 55], thereby enhancing the robustness and accuracy of the final fused graph.

5 Empirical Evaluation

Settings & Vehicle Dataset. We used a *g4dn.12xlarge* instance from AWS Sagemaker to run comparisons. It contains 48 vCPUs and 4 NVIDIA T4 GPUs. We used a combination of F1-Score, Precision, and Recall with different averaging methods [54] to compare results. We evaluated our method on a real-world vehicular test set of $m = 300,000$ sequences, with $|\mathbb{Y}| = 474$ different error patterns and $|\mathbb{X}| = 29,100$ different DTCs forming sequences of $\approx 100 \pm 35$ events. We used Tf_x and Tf_y with 90m and 15m parameters [28]. The two NADEs didn’t see the test set during training. Domain experts manually define error patterns as Boolean rules among DTCs (Fig. 3). We set the elements of this rule as the correct Markov Boundary for each label y_j in the tested sequences.

Multi-label Causal Discovery Comparisons. We benchmark CARGO against local structure learning (LSL) algorithms that estimate Markov Boundaries. This includes established approaches such as CMB [9], MB-by-MB [49], PCD-by-PCD [51], IAMB [47] from the *PyCausalFS* package [52], as well as the more recent, state-of-the-art MI-MCF [26]. 6 random folds of the test data were created and converted into a multi-one-hot data-frame where one row represents one sequence, and each column represents an event type or label (\mathbb{X}, \mathbb{Y}).

Ablation on Aggregation Criterions for Phase 2. We provide an Ablation of the different criteria used in the structural fusion of Markov Boundaries. Union stands for a simple union over all edges without any removal. Frequency or edge voting, counts how often is $X_i \in \text{MB}(Y_j)$. Then apply a static frequency threshold $\tau = [0.05, 0.25, 0.5, 0.8]$. MI uses the mutual information between events and labels as a criterion in a Background Equivalence Search [2]. Expected FPR (false positive ratio) [8] describes two beta distributions which are fitted using the distribution of the mutual information $I(X_i, Y_j)$ extracted from Phase 1. The lower tail is used for outlier detection. Different FPR are chosen $\beta = [0.01, 0.05, 0.15, 0.2]$. Detailed definitions can be found in Appendix C.4.

5.1 Results

Comparisons. We performed comparisons on Table 1 with $n = 50,000$ random sequences. We found that even under this reduced setup, LSL algorithms failed to compute the Markov Boundaries within 3 days (a 3-day timeout), far exceeding practical deployment limits. This behavior highlights the current infeasibility of multi-label causal discovery in high-dimensional event sequences. Current algorithms are cursed under high-dimensional data, since they rely on expensive CI testing that scales

quadratically with the number of nodes [12]. This positions CARGO as a more feasible approach for large-scale, multi-label causal discovery.

Table 1: Comparisons of **MB** retrieval with $m = 50,000$ samples averaged over 6-folds with $|Y| = 474$, $|X| = 29,100$ nodes. Averaging is 'weighted'. The symbol '-' indicates that the algorithm didn't output the **MBs** within 3 days. Metrics are given in %.

Algorithm	Precision \uparrow	Recall \uparrow	F1 \uparrow	Running Time (min) \downarrow
IAMB	-	-	-	> 4320
CMB	-	-	-	> 4320
MB-by-MB	-	-	-	> 4320
PCDbyPCD	-	-	-	> 4320
MI-MCF	-	-	-	> 4320
CARGO	60.6 \pm 1.5	45.8 \pm 1.7	45.8 \pm 1.2	11.7

Criteria. Figure 4 illustrates the impact of aggregation choices during Phase 2. A naïve Union maximizes recall (84% for weighted) but suffers from poor precision. When optimizing a local scoring criterion based on the mutual information BES mi, it didn't significantly improve performance over a basic Union.

Moreover, instead of optimizing a score, fitting Beta distributions to detect outliers using their mutual information appears to perform better; hence, frequency beta outperforms alternatives, particularly in terms of lower FPR. Frequency approaches with a static threshold confirms the analysis in Section 4.1. When a large number of samples per class m_j is available, the frequency cut-off τ needs to be lower to not penalize classes with big support. Thus, we see that frequency with $\tau = [0.5, 0.8]$ have the lower weighted f1 score of all criterions. On the other hand, a small cut-off $\tau = [0.05, 0.25]$ enables a huge improvement in the weighted average (+40% precision), but decrease its macro average metrics (-20% in precision).

Finally, our adaptive thresholding criterion leverages a small threshold for big supports and a big threshold for small supports, which takes advantage of the long-tail distribution. As a result, it is first on both averaging, with respectively 44.88% and 40.9% for weighted and macro f1 score, and 62.8% and 66.1% for weighted and macro precision.

6 Conclusion

We introduced CARGO, a novel framework for multi-label causal discovery in high-dimensional event sequences. By combining one-shot causal discovery with adaptive frequency-aware aggregation, CARGO successfully recovers interpretable causal structures from noisy observational data—achieving results in minutes where classical methods fail to scale.

CARGO could scale further by leveraging general-purpose foundation models for sequences (e.g., time-series transformers pretrained across domains). Such models could extend the applicability beyond automotive diagnostics to healthcare, cybersecurity, and other structured domains.

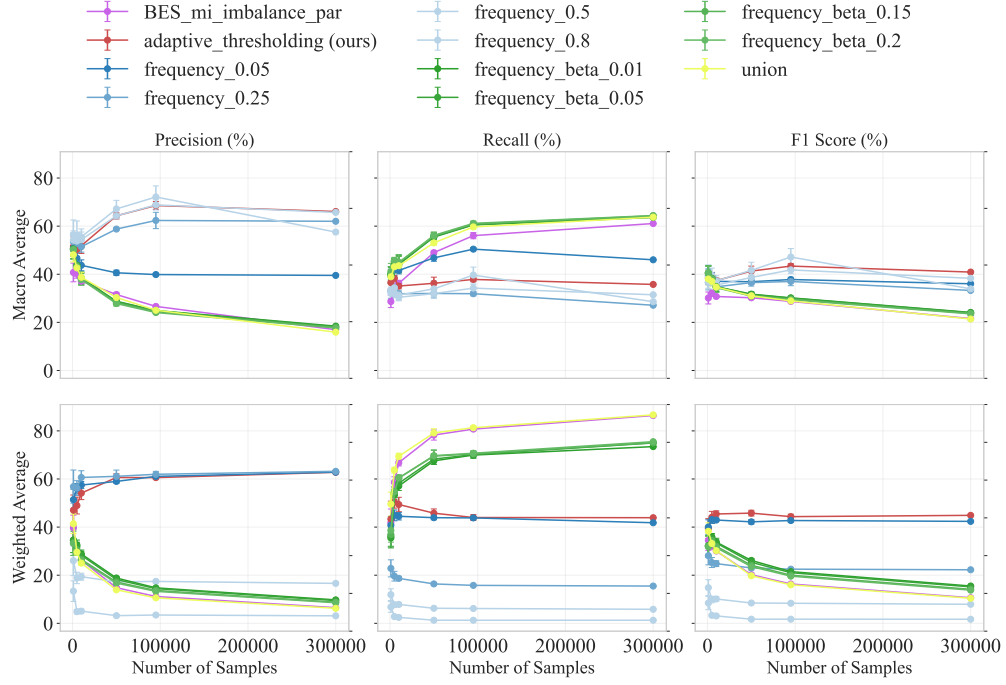
Under the temporal assumptions, large samples, faithfulness, and perfect CI-tests, CARGO recovers the true set of Markov Boundaries. However, we underlined the practical limitations, in particular, long-tail distributions, a common trait in high-dimensional labeled data. Future work should extend this framework to support event-to-event causality and, if possible, relax assumptions such as bounded lagged effects or temporal precedence.

Ultimately, CARGO demonstrates how structured probabilistic methods can bridge the gap between causal discovery theory and scalable, practical deployment in complex industrial systems.

References

[1] L. Breiman. Random forests. *Mach. Learn.*, 45(1):5–32, Oct. 2001. ISSN 0885-6125. doi: 10.1023/A:1010933404324. URL <https://doi.org/10.1023/A:1010933404324>.

Figure 4: Comparison of different criteria for the structural fusion (Phase 2) in function of the number of samples m . With $|Y| = 474$, $|X| = 29,100$ nodes.



- [2] D. M. Chickering. Optimal structure identification with greedy search. *J. Mach. Learn. Res.*, 3(null):507–554, Mar. 2003. ISSN 1532-4435. doi: 10.1162/153244303321897717. URL <https://doi.org/10.1162/153244303321897717>.
- [3] T. Cover. *Elements of Information Theory*. Wiley series in telecommunications and signal processing. Wiley-India, 1999. ISBN 9788126508143. URL <https://books.google.de/books?id=3yGJrqyanyYC>.
- [4] T. Cover and J. Thomas. *Elements of Information Theory*. Wiley-Interscience, 2 edition, 2006. URL <https://www.amazon.com/Elements-Information-Theory-Thomas-Cover/dp/0471241954>.
- [5] J. del Sagrado and S. Moral. *Qualitative Aggregation of Bayesian Networks*, pages 91–108. Springer Vienna, Vienna, 2001. ISBN 978-3-7091-2580-9. doi: 10.1007/978-3-7091-2580-9_5. URL https://doi.org/10.1007/978-3-7091-2580-9_5.
- [6] S. Dong, M. Sebag, K. Uemura, A. Fujii, S. Chang, Y. Koyanagi, and K. Maruhashi. DCILP: A distributed approach for large-scale causal structure learning. In T. Walsh, J. Shah, and Z. Kolter, editors, *AAAI-25, Sponsored by the Association for the Advancement of Artificial Intelligence, February 25 - March 4, 2025, Philadelphia, PA, USA*, pages 16345–16353. AAAI Press, 2025. doi: 10.1609/AAAI.V39I15.33795. URL <https://doi.org/10.1609/aaai.v39i15.33795>.
- [7] A. Doucet, N. de Freitas, and N. Gordon. *An Introduction to Sequential Monte Carlo Methods*, pages 3–14. Springer New York, New York, NY, 2001. ISBN 978-1-4757-3437-9. doi: 10.1007/978-1-4757-3437-9_1. URL https://doi.org/10.1007/978-1-4757-3437-9_1.
- [8] H. Fröhlich and G. W. Klau. Reconstructing Consensus Bayesian Network Structures with Application to Learning Molecular Interaction Networks. In T. Beißbarth, M. Kollmar, A. Leha, B. Morgenstern, A.-K. Schultz, S. Waack, and E. Wingender, editors, *German Conference on Bioinformatics 2013*, volume 34 of *Open Access Series in Informatics (OASIcs)*, pages 46–55, Dagstuhl, Germany, 2013. Schloss Dagstuhl – Leibniz-Zentrum für Informatik. ISBN

978-3-939897-59-0. doi: 10.4230/OASIcs.GCB.2013.46. URL <https://drops.dagstuhl.de/entities/document/10.4230/OASIcs.GCB.2013.46>.

- [9] T. Gao and Q. Ji. Local causal discovery of direct causes and effects. In C. Cortes, N. Lawrence, D. Lee, M. Sugiyama, and R. Garnett, editors, *Advances in Neural Information Processing Systems*, volume 28. Curran Associates, Inc., 2015. URL https://proceedings.neurips.cc/paper_files/paper/2015/file/fcd6e191893e705819b177cddea0-Paper.pdf.
- [10] S. Garrido, S. Borysov, J. Rich, and F. Pereira. Estimating causal effects with the neural autoregressive density estimator. *Journal of Causal Inference*, 9(1):211–228, 2021. doi: doi: 10.1515/jci-2020-0007. URL <https://doi.org/10.1515/jci-2020-0007>.
- [11] J. Go and T. Isaac. Robust expected information gain for optimal bayesian experimental design using ambiguity sets. In *The 38th Conference on Uncertainty in Artificial Intelligence*, 2022. URL <https://openreview.net/forum?id=HU9Ix08oqlc>.
- [12] C. Gong, C. Zhang, D. Yao, J. Bi, W. Li, and Y. Xu. Causal discovery from temporal data: An overview and new perspectives. *ACM Comput. Surv.*, 57(4), Dec. 2024. ISSN 0360-0300. doi: 10.1145/3705297. URL <https://doi.org/10.1145/3705297>.
- [13] X. Guo, K. Yu, L. Liu, and J. Li. Fedcsl: A scalable and accurate approach to federated causal structure learning. *Proceedings of the AAAI Conference on Artificial Intelligence*, 38(11):12235–12243, Mar. 2024. doi: 10.1609/aaai.v38i11.29113. URL <https://ojs.aaai.org/index.php/AAAI/article/view/29113>.
- [14] U. Hasan, E. Hossain, and M. O. Gani. A survey on causal discovery methods for i.i.d. and time series data. *Transactions on Machine Learning Research*, 2023. ISSN 2835-8856. URL <https://openreview.net/forum?id=YdMrdhGx9y>. Survey Certification.
- [15] W. He, X. Mao, C. Ma, Y. Huang, J. M. Hernández-Lobato, and T. Chen. Bsoda: A bipartite scalable framework for online disease diagnosis. In *Proceedings of the ACM Web Conference 2022, WWW ’22*, page 2511–2521, New York, NY, USA, 2022. Association for Computing Machinery. ISBN 9781450390965. doi: 10.1145/3485447.3512123. URL <https://doi.org/10.1145/3485447.3512123>.
- [16] J. A. Hoeting, D. Madigan, A. E. Raftery, and C. T. Volinsky. Bayesian model averaging: a tutorial. *Statistical Science*, 14(4):382–417, 1999.
- [17] A. Holtzman, J. Buys, L. Du, M. Forbes, and Y. Choi. The curious case of neural text degeneration. In *International Conference on Learning Representations*, 2020. URL <https://openreview.net/forum?id=rygGQyrFvH>.
- [18] D. Janzing, D. Balduzzi, M. Grosse-Wentrup, and B. Schölkopf. Quantifying causal influences. *The Annals of statistics*, 41(5):2324–2358, 2013. ISSN 0090-5364.
- [19] A. Kraskov, H. Stögbauer, and P. Grassberger. Estimating mutual information. *Phys. Rev. E*, 69:066138, Jun 2004. doi: 10.1103/PhysRevE.69.066138. URL <https://link.aps.org/doi/10.1103/PhysRevE.69.066138>.
- [20] A. Labach, A. Pokhrel, X. S. Huang, S. Zuberi, S. E. Yi, M. Volkovs, T. Poutanen, and R. G. Krishnan. Duett: Dual event time transformer for electronic health records. In K. Deshpande, M. Fiterau, S. Joshi, Z. Lipton, R. Ranganath, I. Urteaga, and S. Yeung, editors, *Proceedings of the 8th Machine Learning for Healthcare Conference*, volume 219 of *Proceedings of Machine Learning Research*, pages 403–422. PMLR, 11–12 Aug 2023. URL <https://proceedings.mlr.press/v219/1abach23a.html>.
- [21] J. D. Laborda, P. Torrijos, J. M. Puerta, and J. A. Gámez. A ring-based distributed algorithm for learning high-dimensional bayesian networks. In *Symbolic and Quantitative Approaches to Reasoning with Uncertainty: 17th European Conference, ECSQARU 2023, Arras, France, September 19–22, 2023, Proceedings*, page 123–135, Berlin, Heidelberg, 2023. Springer-Verlag. ISBN 978-3-031-45607-7. doi: 10.1007/978-3-031-45608-4_10. URL https://doi.org/10.1007/978-3-031-45608-4_10.

[22] J. D. Lafferty, A. McCallum, and F. C. N. Pereira. Conditional random fields: Probabilistic models for segmenting and labeling sequence data. In *Proceedings of the Eighteenth International Conference on Machine Learning, ICML '01*, page 282–289, San Francisco, CA, USA, 2001. Morgan Kaufmann Publishers Inc. ISBN 1558607781.

[23] J. Li, K. Cheng, S. Wang, F. Morstatter, R. P. Trevino, J. Tang, and H. Liu. Feature selection: A data perspective. *CoRR*, abs/1601.07996, 2016. URL <http://arxiv.org/abs/1601.07996>.

[24] M. Liu, C.-W. Lee, X. Sun, X. Yu, Y. QIAO, and Y. Wang. Learning causal alignment for reliable disease diagnosis. In *The Thirteenth International Conference on Learning Representations*, 2025. URL <https://openreview.net/forum?id=ozZG5FXuTV>.

[25] Q. Luo, L. Zhang, Z. Xing, H. Xia, and Z.-X. Chen. Causal discovery of flight service process based on event sequence. *Journal of Advanced Transportation*, 2021(1):2869521, 2021. doi: <https://doi.org/10.1155/2021/2869521>. URL <https://onlinelibrary.wiley.com/doi/abs/10.1155/2021/2869521>.

[26] L. Ma, L. Hu, Y. Li, W. Ding, and W. Gao. Mi-mcf: A mutual information-based multilabel causal feature selection. *IEEE Transactions on Neural Networks and Learning Systems*, pages 1–15, 2025. doi: 10.1109/TNNLS.2025.3556128.

[27] L. D. Manocchio, S. Layeghy, W. W. Lo, G. K. Kulatilleke, M. Sarhan, and M. Portmann. Flowtransformer: A transformer framework for flow-based network intrusion detection systems. *Expert Systems with Applications*, 241:122564, 2024. ISSN 0957-4174. doi: <https://doi.org/10.1016/j.eswa.2023.122564>. URL <https://www.sciencedirect.com/science/article/pii/S095741742303066X>.

[28] H. Math, R. Lienhart, and R. Schön. Harnessing event sensory data for error pattern prediction in vehicles: A language model approach. *Proceedings of the AAAI Conference on Artificial Intelligence*, 39(18):19423–19431, Apr. 2025. doi: 10.1609/aaai.v39i18.34138. URL <https://ojs.aaai.org/index.php/AAAI/article/view/34138>.

[29] A. McCallum, D. Freitag, and F. C. N. Pereira. Maximum entropy markov models for information extraction and segmentation. In *Proceedings of the Seventeenth International Conference on Machine Learning, ICML '00*, page 591–598, San Francisco, CA, USA, 2000. Morgan Kaufmann Publishers Inc. ISBN 1558607072.

[30] E. Mokhtarian, S. Akbari, A. Ghassami, and N. Kiyavash. A recursive markov boundary-based approach to causal structure learning. In T. D. Le, J. Li, G. Cooper, S. Triantafyllou, E. Bareinboim, H. Liu, and N. Kiyavash, editors, *Proceedings of The KDD'21 Workshop on Causal Discovery*, volume 150 of *Proceedings of Machine Learning Research*, pages 26–54. PMLR, 15 Aug 2021. URL <https://proceedings.mlr.press/v150/mokhtarian21a.html>.

[31] A. Paszke, S. Gross, F. Massa, A. Lerer, J. Bradbury, G. Chanan, T. Killeen, Z. Lin, N. Gimelshein, L. Antiga, A. Desmaison, A. Köpf, E. Yang, Z. DeVito, M. Raison, A. Tejani, S. Chilamkurthy, B. Steiner, L. Fang, J. Bai, and S. Chintala. *PyTorch: an imperative style, high-performance deep learning library*. Curran Associates Inc., Red Hook, NY, USA, 2019.

[32] J. M. Peña. Finding consensus bayesian network structures. *J. Artif. Int. Res.*, 42(1):661–687, Sept. 2011. ISSN 1076-9757.

[33] J. Pearl. *Probabilistic Reasoning in Intelligent Systems: Networks of Plausible Inference*. Morgan Kaufmann Publishers Inc., San Francisco, CA, USA, 1988. ISBN 1558604790.

[34] P. Pirasteh, S. Nowaczyk, S. Pashami, M. Löwenadler, K. Thunberg, H. Ydreskog, and P. Berck. Interactive feature extraction for diagnostic trouble codes in predictive maintenance: A case study from automotive domain. In *Proceedings of the Workshop on Interactive Data Mining*, WIDM'19, New York, NY, USA, 2019. Association for Computing Machinery. ISBN 9781450362962. doi: 10.1145/3304079.3310288. URL <https://doi.org/10.1145/3304079.3310288>.

[35] J. M. Puerta, J. A. Aledo, J. A. Gámez, and J. D. Laborda. Efficient and accurate structural fusion of bayesian networks. *Information Fusion*, 66:155–169, 2021. ISSN 1566-2535. doi: <https://doi.org/10.1016/j.inffus.2020.09.003>. URL <https://www.sciencedirect.com/science/article/pii/S156625352030364X>.

[36] J. Qiao, R. Cai, S. Wu, Y. Xiang, K. Zhang, and Z. Hao. Structural hawkes processes for learning causal structure from discrete-time event sequences. In *Proceedings of the Thirty-Second International Joint Conference on Artificial Intelligence, IJCAI '23*, 2023. ISBN 978-1-956792-03-4. doi: 10.24963/ijcai.2023/633. URL <https://doi.org/10.24963/ijcai.2023/633>.

[37] J. R. Quinlan. Induction of decision trees. *Machine Learning*, 1:81–106, 1986.

[38] A. Radford, K. Narasimhan, T. Salimans, and I. Sutskever. Improving language understanding by generative pre-training. 2018.

[39] L. Rasmy, Y. Xiang, Z. Xie, C. Tao, and D. Zhi. Med-bert: pre-trained contextualized embeddings on large-scale structured electronic health records for disease prediction. *NPJ Digit Med.* 2021 May 20;4(1):86, abs/2005.12833, 2020. doi: 10.1038/s41746-021-00455-y.

[40] R. Y. Rohekar, Y. Gurwicz, and S. Nisimov. Causal interpretation of self-attention in pre-trained transformers. In *Thirty-seventh Conference on Neural Information Processing Systems*, 2023. URL <https://openreview.net/forum?id=DS4rKyS1YC>.

[41] P. Spirtes and C. Glymour. An algorithm for fast recovery of sparse causal graphs. *Social Science Computer Review*, 9(1):62–72, 1991. doi: 10.1177/089443939100900106. URL <https://doi.org/10.1177/089443939100900106>.

[42] P. Spirtes, C. Glymour, and R. Scheines. Causation, prediction, and search, 2nd edition. In *Causation, Prediction, and Search (Second Edition)*, 2001. URL <https://api.semanticscholar.org/CorpusID:124969922>.

[43] E. Steele and A. Tucker. Consensus and meta-analysis regulatory networks for combining multiple microarray gene expression datasets. *Journal of Biomedical Informatics*, 41(6):914–926, December 2008. ISSN 1532-0464. doi: 10.1016/j.jbi.2008.01.011. URL <https://doi.org/10.1016/j.jbi.2008.01.011>.

[44] P. Torrijos, J. M. Puerta, J. A. Gámez, and J. A. Aledo. Informed greedy algorithm for scalable bayesian network fusion via minimum cut analysis, 2025. URL <https://arxiv.org/abs/2504.00467>.

[45] H. Touvron, T. Lavril, G. Izacard, X. Martinet, M.-A. Lachaux, T. Lacroix, B. Rozière, N. Goyal, E. Hambro, F. Azhar, A. Rodriguez, A. Joulin, E. Grave, and G. Lample. Llama: Open and efficient foundation language models, 2023. URL <https://arxiv.org/abs/2302.13971>.

[46] I. Tsamardinos and C. F. Aliferis. Towards principled feature selection: Relevancy, filters and wrappers. In C. M. Bishop and B. J. Frey, editors, *Proceedings of the Ninth International Workshop on Artificial Intelligence and Statistics*, volume R4 of *Proceedings of Machine Learning Research*, pages 300–307. PMLR, 03–06 Jan 2003. URL <https://proceedings.mlr.press/r4/tsamardinos03a.html>. Reissued by PMLR on 01 April 2021.

[47] I. Tsamardinos, C. Aliferis, and A. Statnikov. Algorithms for large scale markov blanket discovery. pages 376–381, 01 2003.

[48] A. Vaswani, N. Shazeer, N. Parmar, J. Uszkoreit, L. Jones, A. N. Gomez, L. u. Kaiser, and I. Polosukhin. Attention is all you need. In I. Guyon, U. V. Luxburg, S. Bengio, H. Wallach, R. Fergus, S. Vishwanathan, and R. Garnett, editors, *Advances in Neural Information Processing Systems*, volume 30. Curran Associates, Inc., 2017. URL https://proceedings.neurips.cc/paper_files/paper/2017/file/3f5ee243547dee91fdb053c1c4a845aa-Paper.pdf.

[49] C. Wang, Y. Zhou, Q. Zhao, and Z. Geng. Discovering and orienting the edges connected to a target variable in a dag via a sequential local learning approach. *Computational Statistics and Data Analysis*, 77:252–266, 2014. ISSN 0167-9473. doi: <https://doi.org/10.1016/j.csda.2014.03.003>. URL <https://www.sciencedirect.com/science/article/pii/S0167947314000802>.

[50] Z. Wang, P. Ma, and S. Wang. Towards practical federated causal structure learning. In *Machine Learning and Knowledge Discovery in Databases: Research Track: European Conference, ECML PKDD 2023, Turin, Italy, September 18–22, 2023, Proceedings, Part II*, page 351–367, Berlin, Heidelberg, 2023. Springer-Verlag. ISBN 978-3-031-43414-3. doi: 10.1007/978-3-031-43415-0_21. URL https://doi.org/10.1007/978-3-031-43415-0_21.

[51] J. Yin, Y. Zhou, C. Wang, P. He, C. Zheng, and Z. Geng. Partial orientation and local structural learning of causal networks for prediction. In I. Guyon, C. Aliferis, G. Cooper, A. Elisseeff, J.-P. Pellet, P. Spirtes, and A. Statnikov, editors, *Proceedings of the Workshop on the Causation and Prediction Challenge at WCCI 2008*, volume 3 of *Proceedings of Machine Learning Research*, pages 93–105, Hong Kong, 03–04 Jun 2008. PMLR. URL <http://proceedings.mlr.press/v3/yin08a.html>.

[52] K. Yu, X. Guo, L. Liu, J. Li, H. Wang, Z. Ling, and X. Wu. Causality-based feature selection: Methods and evaluations. *ACM Comput. Surv.*, 53(5), Sept. 2020. ISSN 0360-0300. doi: 10.1145/3409382. URL <https://doi.org/10.1145/3409382>.

[53] C. Zhang, G. Almpandis, G. Fan, B. Deng, Y. Zhang, J. Liu, A. Kamel, P. Soda, and J. Gama. A systematic review on long-tailed learning. *IEEE Transactions on Neural Networks and Learning Systems*, PP:1–21, 02 2025. doi: 10.1109/TNNLS.2025.3539314.

[54] M.-L. Zhang and Z.-H. Zhou. A review on multi-label learning algorithms. *Knowledge and Data Engineering, IEEE Transactions on*, 26:1819–1837, 08 2014. doi: 10.1109/TKDE.2013.39.

[55] Q.-C. Zheng, S.-H. Lyu, S.-Q. Zhang, Y. Jiang, and Z.-H. Zhou. On the consistency rate of decision tree learning algorithms. In F. Ruiz, J. Dy, and J.-W. van de Meent, editors, *Proceedings of The 26th International Conference on Artificial Intelligence and Statistics*, volume 206 of *Proceedings of Machine Learning Research*, pages 7824–7848. PMLR, 25–27 Apr 2023. URL <https://proceedings.mlr.press/v206/zheng23b.html>.

A Notations and Definitions

A.1 Notations

We use capital letters (e.g., X) to denote random variables, lower-case letters (e.g., x) for their realisations, and bold capital letters (e.g., \mathbf{X}) for sets of variables. Let \mathbf{U} denote the set of all (discrete) random variables. We define the event set $\mathbf{X} = \{X_1, \dots, X_n\} \subset \mathbf{U}$, and the label set $\mathbf{Y} = \{Y_1, \dots, Y_n\} \subset \mathbf{U}$. When explicitly said, event $X_i^{(t_i)}$ represent the occurrence of X_i at the sequence step i and time t_i . Similarly for $Y_{i+1}^{(t_{i+1})}$.

A.2 Definitions

Definition 1 (Faithfulness). *Spirites et al. [42]. Given a BN $\langle \mathbf{U}, \mathbb{G}, P \rangle$, \mathbb{G} is faithful to P if and only if every conditional independence present in P is entailed by \mathbb{G} and the Markov condition holds. P is faithful if and only if there exist a DAG \mathbb{G} such that \mathbb{G} is faithful to P .*

Definition 2 (Conditional Independence). *Variables X and Y are said to be conditionally independent given a variable set \mathbf{Z} , if $P(X, Y | \mathbf{Z}) = P(X | \mathbf{Z})P(Y | \mathbf{Z})$, denoted as $X \perp Y | \mathbf{Z}$. Inversely, $X \not\perp Y | \mathbf{Z}$ denotes the conditional dependence. Using the conditional mutual information [3] to measure the independence relationship, this implies that $I(X, Y | \mathbf{Z}) = 0 \Leftrightarrow X \perp Y | \mathbf{Z}$.*

Definition 3 (Markov Boundary). *Tsamardinos and Aliferis [46]. In a faithful BN $\langle \mathbf{U}, \mathbb{G}, P \rangle$, for a set of variables $\mathbf{Z} \subset \mathbf{U}$ and label $Y \in \mathbf{U}$, if all other variables $X \in \{\mathbf{X} - \mathbf{Z}\}$ are independent of Y conditioned on \mathbf{Z} , and any proper subset of \mathbf{Z} do not satisfy the condition, then \mathbf{Z} is the Markov Boundary of Y : $\mathbf{MB}(Y)$.*

Definition 4. (Markov Equivalence Class). *Two distinct graphs \mathbb{G}, \mathbb{G}' are said to belong to the same Markov Equivalence Class (MEC) if they have the same set of conditional independencies, i.e $I(\mathbb{G}) = I(\mathbb{G}')$.*

Definition 5. (Decomposable Criterion). *We say that a scoring criterion $S(\mathbb{G}, D)$ is decomposable if it can be written as a sum of measures, each of which is a function only of one node and its parents. In other words, a decomposable scoring criterion S applied to a DAG \mathbb{G} can always be expressed as:*

$$S(\mathbb{G}, \mathbf{D}) = \sum_i^n s(X_i, \mathbf{Pa}_i^{\mathbb{G}}) \quad (11)$$

Definition 6 (Score equivalent). *Chickering [2]. A score S is score equivalent if it assigns the same score to all the graphs in the same MEC.*

Definition 7 (Local Consistency). *Chickering [2] Let \mathbf{D} contain m iid samples from some distribution $p(\cdot)$. Let \mathbb{G} be any possible DAG and \mathbb{G}' a different DAG obtained by adding the edge $i \rightarrow j$ to \mathbb{G} . A score S is locally consistent if both hold:*

- If $X_i \not\perp_p X_j | \mathbf{Pa}_j^{\mathbb{G}}$, then $S(\mathbb{G}', \mathbf{D}) > S(\mathbb{G}, \mathbf{D})$
- If $X_i \perp_p X_j | \mathbf{Pa}_j^{\mathbb{G}}$, then $S(\mathbb{G}', \mathbf{D}) < S(\mathbb{G}, \mathbf{D})$

A.3 Assumptions

Assumption 1 (Temporal Precedence). *Given a perfectly recorded sequence of events $((x_1, t_1), \dots, (x_L, t_L))$ with labels (\mathbf{y}_L, t_L) and monotonically increasing time of occurrence $0 \leq t_1 \leq \dots \leq t_L$, an event x_i is allowed to influence any subsequent event x_j such that $t_i \leq t_j$ and $i < j$. Formally, the graph $\mathbb{G} = (\mathbf{U}, \mathbf{E})$, $(x_i, x_j) \in \mathbf{E} \implies t_i \leq t_j$ and $i < j$*

It allows us to remove ambiguity in causal directionality and is widely used in time-series and sequential data [12].

Assumption 2 (Bounded Lagged Effects). *Once we observed events up to timestamp t_i and step i as $\mathbf{Z}_{\leq t_i} = ((x_1, t_1), \dots, (x_i, t_i))$, any future lagged copy of event $X_i^{(t_i+\tau)}$ is independent of Y_j conditioned on $\mathbf{Z}_{\leq t_i}$:*

$$Y_j \perp X_i^{(t_i+\tau)} | \mathbf{Z}_{\leq t_i}$$

Where $\tau = t_{i+1} - t_i$ is a finite bound on the allowed time delay for causal influence.

In other words, we allow the causal influence of event X_i on Y_j until the next event X_{i+1} is observed. We note that for data with strong lagged effects (e.g., financial transactions), this might not hold well, but for log-based and error code-based data, this is usually correct.

Assumption 3 (Causal Sufficiency for Labels). *All relevant variables are observed, and there are no hidden confounders affecting the labels.*

Assumption 4 (Oracle Models). *We assume that two autoregressive Transformer models, Tf_x and Tf_y , are trained via maximum likelihood on a dataset of multi-labeled event sequences $D = \{S_l^1, \dots, S_l^m\} \subset \mathbb{S}$, and can perfectly approximate the true conditional distributions of events and labels:*

$$P(X_i|Pa(X_i)) = P_{\theta_x}(X_i|Pa(X_i)) = Tf_x(S_{<i}), \quad P(Y_j|Pa(Y_j)) = P_{\theta_y}(Y_j|Pa(Y_j)) = Tf_y(S_{\leq i}) \quad (12)$$

A.4 Lemmas

Lemma 1 (Identifiability of \mathbb{G}). *Assuming the faithfulness condition holds for the true causal graph \mathbb{G} . Let Tf_x and Tf_y be oracle models that model the true conditional distributions of events and labels, respectively. The joint distribution P_{θ_x, θ_y} can then be constructed, and any conditional independence detected from the distributions estimated by Tf_x and Tf_y corresponds to a conditional independence in \mathbb{G} :*

$$X_i \perp_{\theta_x, \theta_y} Y_j | \mathbf{Z} \implies X_i \perp_{\mathbb{G}} Y_j | \mathbf{Z}.$$

Where $\perp_{\theta_x, \theta_y}$ denotes the independence entailed by the joint probability P_{θ_x, θ_y} .

Lemma 2 (Markov Boundary Equivalence). *In a multi-label event sequence S_l and under the temporal precedence assumption A1, the Markov Boundary of each label Y_j is only its parents such that $\forall X \in \{U - Pa(Y_j)\}, X \perp Y_j | Pa(Y_j) \Leftrightarrow MB(Y_j) = Pa(Y_j)$.*

B Proofs

We provide proofs for the results described in Section 3

B.1 Proof of Lemma 1

Proof. We assume that the data is generated by the associated causal graph \mathbb{G} following the sequential BN from a multi-labelled sequence S . And that the faithfulness assumption holds [33], meaning that all conditional independencies in the observational data are implied by the true causal graph \mathbb{G} .

Given that the Oracle models Tf_x and Tf_y are trained to perfectly approximate the true conditional distributions, for any variable U_i in the graph, we have:

$$P(U_i|Pa(U_i)) = \begin{cases} P(Y_j|Pa(Y_j)) = P_{\theta_y}(Y_j|Pa(Y_j)), & \text{if } U_i \in \mathbf{Y} \\ P(X_i|Pa(X_i)) = P_{\theta_x}(X_i|Pa(X_i)), & \text{otherwise.} \end{cases}$$

The joint distribution P_{θ_x, θ_y} can then be constructed using the chain rule $P_{\theta_x, \theta_y}(X_1, \dots, X_i, Y_1, \dots, Y_c) = \prod_{k=0}^i P(X_k|Pa(X_k)) \prod_{l}^c P(Y_l|Pa(Y_l))$. By the faithfulness assumption [33], if the conditional independencies hold in the data, they must also hold in the causal graph \mathbb{G} :

$$X_i \perp Y_j | \mathbf{Z} \implies X_i \perp_{\mathbb{G}} Y_j | \mathbf{Z}$$

Since we can approximate the true conditional distributions, it follows that:

$$X_i \perp_{\theta_x, \theta_y} Y_j | \mathbf{Z} \implies X_i \perp Y_j | \mathbf{Z} \implies X_i \perp_{\mathbb{G}} Y_j | \mathbf{Z}$$

Where $\perp_{\theta_x, \theta_y}$ denotes the independence entailed by the joint probability P_{θ_x, θ_y} . Thus, the graph \mathbb{G} can be identified from the observational data. \square

B.2 Proof of Lemma 2

Proof. Let $\langle U, \mathbb{G}, P \rangle$ be the sequential BN composed of the events from the multi-labeled sequence $S_l = (\{(t_1, x_1, \dots, (t_L, x_L)\}_{i=1}^L, (y_L, t_L)\})$. Following the temporal precedence assumption

A1, the labels y_L can only be caused by past events (x_1, \dots, x_L) ; moreover, by definition, labels do not cause any other labels. Thus, Y_j has no descendants, so no children and spouses. Therefore, together with the Markov Assumption, we know that $\forall X \in \{\mathbf{U} - Pa(Y_j)\} : Y_j \perp X | Pa(Y_j)$. Which is the definition of the MB (Def. 3). Thus, $\mathbf{MB}(Y_j) = Pa(Y_j)$.

□

B.3 Proof of Theorem 1.

Proof. By recurrence over the sequence length L of the multi-label sequence S_l^k , we want to show that under temporal precedence A1, bounded lagged effects A2, causal sufficiency A3, Oracle Models A4 the Markov Boundary of label Y_j can be identified in the causal graph \mathbb{G} .

Let's define \mathcal{M}_j^L as the estimated Markov Boundary of Y_j after observing L events.

Base Case: $L = 1$: Consider the BN for step $L = 1$ following the Markov assumption [33] with two nodes X_1, Y_j . Using Tf_x, Tf_y as Oracle Models A4, we can express the conditional probabilities for any node U :

$$P(U|Pa(U)) = \begin{cases} P(X_1) = P_{\theta_x}(X_1|[CLS]) & \text{if } U \in \mathbf{X} \\ P(Y_j|X_1) = P_{\theta_y}(Y_j|X_1) & \text{otherwise} \end{cases} \quad (13)$$

Assuming that \mathbb{P} is faithful (A1) to \mathbb{G} , no hidden confounders bias the estimate (A3) and temporal precedence (A1), we can estimate the CMI 4 such that $\text{iif } I(X_1, Y_j|\emptyset) > 0 \Leftrightarrow Y_j \not\perp_{\theta_x, \theta_y} X_1 \implies Y_j \not\perp_{\mathbb{G}} X_1$ (Lemma 1).

Since we assume temporal precedence A1, we can orient the edge such that X_1 must be a parent of Y_j in \mathbb{G} . Using Lemma 2, we know that $Par(Y_j) = \mathbf{MB}(Y_j) \implies X_1 \in \mathbf{MB}(Y_j)$, thus we must include X_1 in M_j^1 , otherwise not.

Heredity: For $L = i$, we obtained M_j^i with the sequential BN up to step $L = i$. Now for $L = i + 1$, the sequential BN has $i + 2$ nodes denoted as $\mathbf{U}' = (X_1, \dots, X_i, X_{i+1}, Y_j)$. Using the Oracle Models A4 and following the Markov assumption [33], we can estimate the following conditional probabilities for any nodes $U \in \mathbf{U}'$:

$$P(U|Pa(U)) = \begin{cases} P(Y_j|Pa(Y_j)) \approx P_{\theta_y}(Y_j|Pa(Y_j)), & \text{if } U \in \mathbf{Y} \\ P(X|Pa(X)) \approx P_{\theta_x}(X|Pa(X)), & \text{otherwise.} \end{cases} \quad (14)$$

By bounded lagged effects (A2) we know that the causal influence of past $X_{\leq i}$ on Y_j has expired. Moreover, no hidden confounders (A3) bias the independence testing. Finally, using Eq. (4) we can estimate the CMI such that $\text{iif } I(Y_j, X_{i+1}|\mathbf{Z}) > 0 \Leftrightarrow Y_j \not\perp_{\theta_x, \theta_y} X_{i+1}|\mathbf{Z} \implies Y_j \not\perp_{\mathbb{G}} X_{i+1}|\mathbf{Z}$ (Lemma 1).

Since we assume temporal precedence A1, we can orient the edge so that X_{i+1} must be a parent of Y_j in \mathbb{G} . Using Lemma 2, we know that $Par(Y_j) = \mathbf{MB}(Y_j) \implies X_{i+1} \in \mathbf{MB}(Y_j)$. Thus $X_{i+1} \in M_j^{i+1}$ which represent the $\mathbf{MB}(Y_j)$ for step $i + 1$.

Finally, \mathcal{M}_j^{i+1} still recovers the Markov Boundary of Y_j such that

$$\forall U \in \{\mathbf{U}' - \mathcal{M}_j^{i+1}\}, Y_j \perp U | \mathcal{M}_j^{i+1}$$

□

C Ablations

C.1 NADEs Quality.

We did several ablations on the quality of the NADEs and their impact on the one-shot causal discovery phase. In particular, Table 2 presents multiple Tf_x , Tf_y with respectively 90 and 15 million parameters or 34 and 4 million parameters. We also varied the context window (conditioning set Z), trained on different amounts of data (tokens), and reported the classification results on the test set of Tf_y alone. We didn't output the running time since it was approximately the same for all NADEs: 1.27 minutes of 50,000 samples and 0.14 for 5000.

We observe that scaling up the NADEs model size and the trained data show the most significant improvements. Afterward, it is via the context c , which, after $c = 15$, shows a decline in performance across a larger number of samples. We then choose the backbone with 1.5B Tokens, 105m parameters, and a context $c = 15$ for our experiments.

Table 2: Ablations of the performance of Phase 1 (One-shot **MB** retrieval) in function of different NADEs with $m = 50,000$ and $m = 500$ samples averaged over 6-folds. Classification metrics use weighted averaging. Metrics are given in %.

Tokens	Parameters	Context	Precision (\uparrow)	Recall (\uparrow)	F1 Score (\uparrow)	Tfy	F1 (\uparrow)
<i>For $n = 50,000$ samples</i>							
1.5B	105m	$c = 4$	47.95 ± 1.05	30.65 ± 0.51	37.39 ± 0.67		88.6
1.5B	105m	$c = 12$	54.62 ± 1.03	29.88 ± 0.73	38.63 ± 0.85		90.43
1.5B	105m	$c = 15$	55.26 ± 1.42	31.37 ± 0.82	40.02 ± 1.03		90.57
1.5B	105m	$c = 20$	49.52 ± 1.59	31.76 ± 0.85	36.54 ± 1.10		91.19
1.5B	105m	$c = 30$	36.65 ± 1.18	22.75 ± 0.78	26.57 ± 0.91		92.64
300m	47m	$c = 20$	39.49 ± 1.77	26.30 ± 0.89	29.01 ± 1.10		83.6
<i>For $n = 500$ samples</i>							
1.5B	105m	$c = 12$	54.84 ± 4.55	31.45 ± 2.23	39.95 ± 2.83		90.43
1.5B	105m	$c = 15$	55.04 ± 3.36	29.90 ± 1.78	38.74 ± 2.24		90.57
1.5B	105m	$c = 20$	48.84 ± 4.01	31.65 ± 2.37	36.19 ± 2.65		91.19
300m	47m	$c = 20$	38.23 ± 2.91	25.31 ± 2.39	27.92 ± 2.25		83.6

C.2 Sampling Number

We tested different values of N for the sampling method across averaging methods (micro, macro, weighted), as shown in Fig. 5. We performed eight different runs and reported the average, standard deviation, and elapsed time. In general, sampling with a larger N tends to reduce the standard deviation and yield more reliable Markov Boundary estimates. Moreover, as we process more samples, the model gradually improves, following a logarithmic growth pattern until it converges to a final score. We also verify that our time complexity is linear with the number of samples N . Based on these results, we generally select $N = 68$ as the sample size.

C.3 Dynamic Thresholding

We performed ablations on the effect of k during the dynamic thresholding of the CMI (Eq. (9)) to access conditional independence in Fig. 6. To balance the classification metrics across the different averaging, we set $k = 2.75$.

Figure 5: Evolution of several classification metrics (one-shot) and elapsed time per sample in function of the number of samples N chosen. Results are reported using 1-sigma error bar.

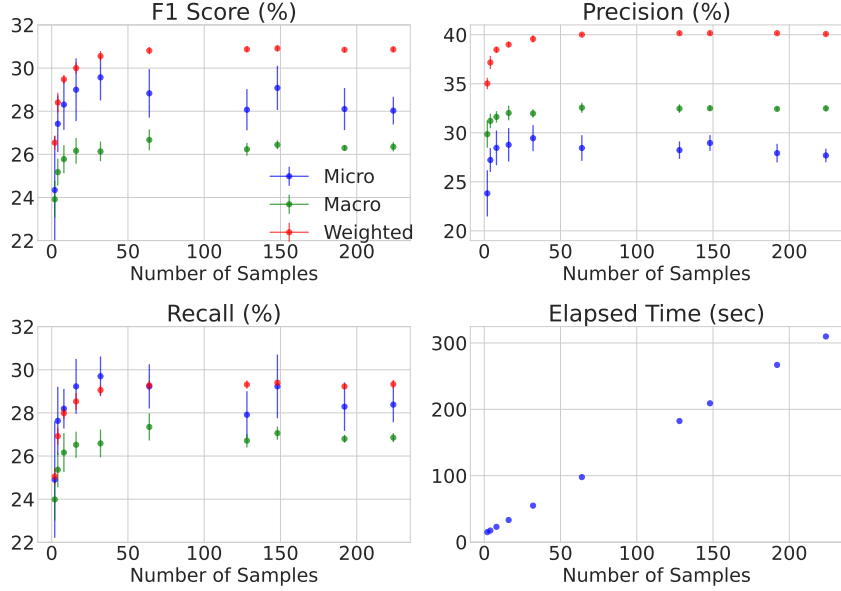
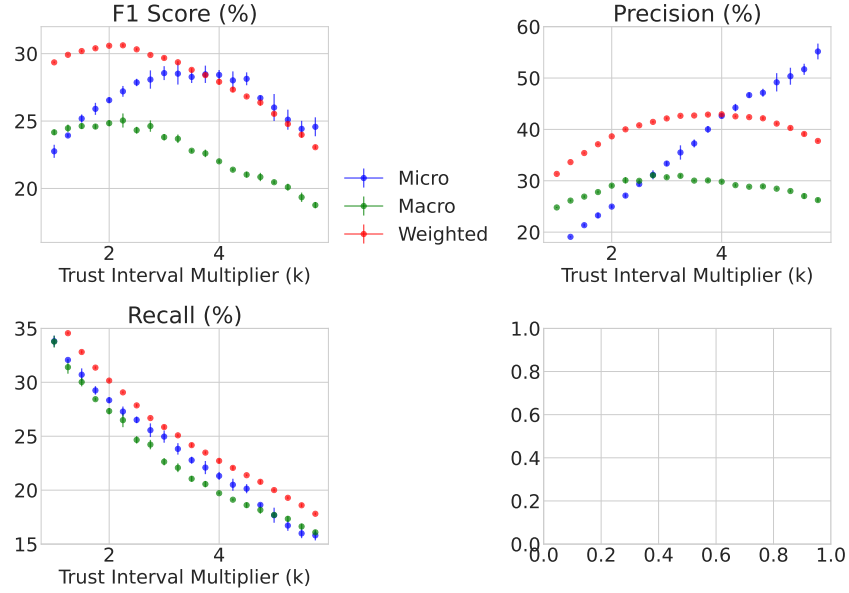


Figure 6: Evolution of one-shot F1 Score, Precision, and Recall in function of coefficient k . Results are reported using 1-sigma error bar.



C.4 Criterions

This section presents the different criteria used for comparison in the experimental evaluation.

C.5 Frequency

Frequency-based heuristics that apply fixed thresholds τ to the empirical frequency of the occurrence of X_i in each of the Markov Boundary $\mathbf{MB}(Y_j)$. Formally, For each label Y_j , after merging all local edge sets into a global set $E = \bigcup_{i=1}^m E_i$, we evaluate each candidate variable $X_i \in \mathbf{MB}_j$ based on

its frequency of appearance across the local models. If this frequency exceeds the threshold τ , the variable is retained in the final merged \mathbf{MB}_j ; otherwise, it is discarded.

C.5.1 Expected FPR Adjustment

Same principle as in [8] except that we fit the two Beta distributions on the mutual information of $I(Y_j, X_i)$ instead of the raw frequencies.

C.5.2 Mutual Information

BES The BES is the second phase of GES [2], where edges are removed one after the other to maximize a criterion S . Heuristics approaches [35, 5] aim to solve this problem by optimizing:

$$E = \arg \max_{E_i \in \varepsilon} \sum_{e \in E_i} S(e) \quad (15)$$

Where ε denotes the search space (all possible edges over \mathbf{U}) and $S(e)$ a criterion function for edge relevance (e.g. edge frequency, thresholds, \dots). This formulation takes into account the underlying edges' characteristics but not the overall network structure, complexity and missing data [32], leading to a *consensus fusion approach* [44].

Estimating Mutual Information in Event Sequences. We want to reuse the estimated conditional mutual information, Eq. (4), and profit from the parallelized inference of Phase 1 (Fig. 2).

As argued out by Janzing et al. [18], a causal strength measure (or criterion) $C_{X_i \rightarrow Y_j}$ should possess multiple properties. Notably, if $C_{X_i \rightarrow Y_j} = 0$, then the joint distribution satisfies the Markov condition with respect to the DAG obtained by removing the arrow $X_i \rightarrow Y_j$. Moreover, the true DAG reads $X_i \rightarrow Y$ iff $C_{X_i \rightarrow Y_j} = I(X_i, Y_j)$.

It is a natural criterion for merging edges across multiple causal graphs. However, it remains tricky to estimate [19]. Using the chain rule of conditional mutual information [3], we can rewrite it as:

$$I(Y_j, X_i | \mathbf{Z}) = I(Y_j, X_i) - I(Y_j, X_i, \mathbf{Z}) \quad (16)$$

Where $I(Y_j, X_i, \mathbf{Z})$ is the interaction information [4], which tells us whether knowing \mathbf{Z} explains away the dependency between X_i and Y_j (negative interaction), or enhances it (positive interaction):

$$I(Y_j, X_i, \mathbf{Z}) \triangleq I(Y_j, \mathbf{Z}) - I(Y_j, \mathbf{Z} | X_i)$$

$I(Y_j, \mathbf{Z})$ can be estimated using the same Monte-Carlo sampling as for $I(Y_j, X_i | \mathbf{Z})$ (4). Since $I(Y_j, \mathbf{Z}) = H(Y_j) - H(Y | \mathbf{Z}_j)$, the marginal $p(y)$ is needed. Fortunately, the dataset \mathbf{D} is large enough, hence the frequencies of y_j are recovered empirically and an estimate $\hat{p}(y)$ which we assume to be equal to the true marginal $p(y)$. We acknowledge that under a restricted dataset, $\hat{p}(y)$ might differ from $p(y)$. This yields to:

$$I(Y_j, \mathbf{Z}) = \mathbb{E}_z D_{KL}(P(Y_j | \mathbf{Z}) || \hat{P}(Y_j)) = \mathbb{E}_z I_G(Y_j, z) \quad (17)$$

Formally, we assume that for long sequences i.e $i \rightarrow +\infty$, our event sequences form a stationary ergodic stochastic process and $I(Y_j, \mathbf{Z} | X_i)$ is negligible compare to $I(Y_j, \mathbf{Z})$ since \mathbf{Z} is containing most of the information to predict Y_j . This reduces the mutual information to

$$I(Y_j, X_i) \approx I(Y_j, X_i | \mathbf{Z}) + I(Y_j | \mathbf{Z})$$

Criterion. We propose a **Class-Aware Information Gain (CAIG)** score for evaluating candidate edges during Phase 2 of CARGO. Given m i.i.d. samples from a dataset \mathbf{D} , CAIG balances three key factors: mutual information derived from information gain, class imbalance, and network complexity.

For each label node Y_j , with candidate parent set $\mathbf{Pa}_j^{\mathbb{G}}$, the CAIG score is:

$$S(\mathbb{G}', \mathbf{D}) = \sum_{j=1}^n s_I(Y_j, \mathbf{Pa}_j^{\mathbb{G}}) - \alpha \cdot |\mathbf{Pa}_j^{\mathbb{G}}| \cdot \log \left(\frac{m}{m_j} + 1 \right) \quad (18)$$

With $s_I(Y_j, \mathbf{Pa}_j^{\mathbb{G}}) = \sum_{X_i \in \mathbf{Pa}_j^{\mathbb{G}}} I(Y_j, X_i)$, α is a regularization hyperparameter, m_j is the number of positive instances for class Y_j .

This formulation encourages informative yet parsimonious graph structures, correcting for underrepresented labels via the regularization term. It is also efficient since CAIG is decomposable [2] like BIC with the local s_I . This criterion is denoted as BES mi imbalance par in our experiments in Fig. 4.

D Implementation

D.1 Computation.

A key advantage of our approach is its scalability. Unlike traditional methods whose complexity depends on the event and label cardinality $|\mathbb{X}|$ and $|\mathbb{Y}|$ [23], our method is agnostic to both. As illustrated in Figure 2, all steps are parallelized on GPUs. CMI estimations are independently performed for all positions $i \in [c, L]$, with the sampling pushed into the batch dimension and results averaged across labels, leading to $BS \times N \times L$ CI-tests per batch $D = \{S_l^0, \dots, S_l^m\}$. Consequently, time complexity transitions from $\mathcal{O}(BS \times N \times L)$ to $\mathcal{O}(1)$ per batch due to GPU parallelism. The complexity is bounded by the Transformers’ inference part, where it scales quadratically with the sequence length $\mathcal{O}(L^2)$ if one uses vanilla self-attention [48].

D.2 Phase 1

The following is the implementation of the one-shot phase in PyTorch [31].

```

1 def topk_p_sampling(z, prob_x, c: int, n: int = 64, p: float = 0.8, k:
2                         int = 35,                               cls_token_id: int = 1, temp: float = None):
3     # Sample just the context
4     input_ = prob_x[:, :c]
5
6     # Top-k first
7     topk_values, topk_indices = torch.topk(input_, k=k, dim=-1)
8
9     # Top-p over top-k values
10    sorted_probs, sorted_idx = torch.sort(topk_values, descending=True
11                                           , dim=-1)
12    cum_probs = torch.cumsum(sorted_probs, dim=-1)
13    mask = cum_probs > p
14
15    # Ensure at least one token is kept
16    mask[..., 0] = 0
17
18    # Mask and normalize
19    filtered_probs = sorted_probs.masked_fill(mask, 0.0)
20    filtered_probs += 1e-8 # for numerical stability
21    filtered_probs /= filtered_probs.sum(dim=-1, keepdim=True)
22
23    # Unscramble to match the original top-k indices
24    # Need to reorder the sorted indices back to the original top-k
25    reorder_idx = torch.argsort(sorted_idx, dim=-1)
26    filtered_probs = torch.gather(filtered_probs, -1, reorder_idx)
27
28    batched_probs = filtered_probs.unsqueeze(1).repeat(1, n, 1, 1)
29    # (bs, n, seq_len, k)
30    batched_indices = topk_indices.unsqueeze(1).repeat(1, n, 1, 1)
31    # (bs, n, seq_len, k)
32
33    sampled_idx = torch.multinomial(batched_probs.view(-1, k), 1)
34    # (bs*n*seq_len, 1)
35    sampled_idx = sampled_idx.view(-1, n, c).unsqueeze(-1)
36
37
38
39
40
41
42
43
44
45
46
47
48
49
50
51
52
53
54
55
56
57
58
59
60
61
62
63
64
65
66
67
68
69
70
71
72
73
74
75
76
77
78
79
80
81
82
83
84
85
86
87
88
89
90
91
92
93
94
95
96
97
98
99
100
101
102
103
104
105
106
107
108
109
110
111
112
113
114
115
116
117
118
119
120
121
122
123
124
125
126
127
128
129
130
131
132
133
134
135
136
137
138
139
140
141
142
143
144
145
146
147
148
149
150
151
152
153
154
155
156
157
158
159
160
161
162
163
164
165
166
167
168
169
170
171
172
173
174
175
176
177
178
179
180
181
182
183
184
185
186
187
188
189
190
191
192
193
194
195
196
197
198
199
200
201
202
203
204
205
206
207
208
209
210
211
212
213
214
215
216
217
218
219
220
221
222
223
224
225
226
227
228
229
230
231
232
233
234
235
236
237
238
239
240
241
242
243
244
245
246
247
248
249
250
251
252
253
254
255
256
257
258
259
260
261
262
263
264
265
266
267
268
269
270
271
272
273
274
275
276
277
278
279
280
281
282
283
284
285
286
287
288
289
290
291
292
293
294
295
296
297
298
299
300
301
302
303
304
305
306
307
308
309
310
311
312
313
314
315
316
317
318
319
320
321
322
323
324
325
326
327
328
329
330
331
332
333
334
335
336
337
338
339
340
341
342
343
344
345
346
347
348
349
350
351
352
353
354
355
356
357
358
359
360
361
362
363
364
365
366
367
368
369
370
371
372
373
374
375
376
377
378
379
380
381
382
383
384
385
386
387
388
389
390
391
392
393
394
395
396
397
398
399
400
401
402
403
404
405
406
407
408
409
410
411
412
413
414
415
416
417
418
419
420
421
422
423
424
425
426
427
428
429
430
431
432
433
434
435
436
437
438
439
440
441
442
443
444
445
446
447
448
449
450
451
452
453
454
455
456
457
458
459
460
461
462
463
464
465
466
467
468
469
470
471
472
473
474
475
476
477
478
479
480
481
482
483
484
485
486
487
488
489
490
491
492
493
494
495
496
497
498
499
500
501
502
503
504
505
506
507
508
509
510
511
512
513
514
515
516
517
518
519
520
521
522
523
524
525
526
527
528
529
530
531
532
533
534
535
536
537
538
539
540
541
542
543
544
545
546
547
548
549
550
551
552
553
554
555
556
557
558
559
560
561
562
563
564
565
566
567
568
569
570
571
572
573
574
575
576
577
578
579
580
581
582
583
584
585
586
587
588
589
589
590
591
592
593
594
595
596
597
598
599
600
601
602
603
604
605
606
607
608
609
610
611
612
613
614
615
616
617
618
619
620
621
622
623
624
625
626
627
628
629
630
631
632
633
634
635
636
637
638
639
640
641
642
643
644
645
646
647
648
649
650
651
652
653
654
655
656
657
658
659
660
661
662
663
664
665
666
667
668
669
670
671
672
673
674
675
676
677
678
679
680
681
682
683
684
685
686
687
688
689
690
691
692
693
694
695
696
697
698
699
700
701
702
703
704
705
706
707
708
709
710
711
712
713
714
715
716
717
718
719
720
721
722
723
724
725
726
727
728
729
729
730
731
732
733
734
735
736
737
738
739
739
740
741
742
743
744
745
746
747
748
749
749
750
751
752
753
754
755
756
757
758
759
759
760
761
762
763
764
765
766
767
768
769
769
770
771
772
773
774
775
776
777
778
779
779
780
781
782
783
784
785
786
787
787
788
789
789
790
791
792
793
794
795
796
797
797
798
799
799
800
801
802
803
804
805
806
807
808
809
809
810
811
812
813
814
815
816
817
817
818
819
819
820
821
822
823
824
825
825
826
827
827
828
829
829
830
831
831
832
833
833
834
835
835
836
836
837
837
838
838
839
839
840
840
841
841
842
842
843
843
844
844
845
845
846
846
847
847
848
848
849
849
850
850
851
851
852
852
853
853
854
854
855
855
856
856
857
857
858
858
859
859
860
860
861
861
862
862
863
863
864
864
865
865
866
866
867
867
868
868
869
869
870
870
871
871
872
872
873
873
874
874
875
875
876
876
877
877
878
878
879
879
880
880
881
881
882
882
883
883
884
884
885
885
886
886
887
887
888
888
889
889
890
890
891
891
892
892
893
893
894
894
895
895
896
896
897
897
898
898
899
899
900
900
901
901
902
902
903
903
904
904
905
905
906
906
907
907
908
908
909
909
910
910
911
911
912
912
913
913
914
914
915
915
916
916
917
917
918
918
919
919
920
920
921
921
922
922
923
923
924
924
925
925
926
926
927
927
928
928
929
929
930
930
931
931
932
932
933
933
934
934
935
935
936
936
937
937
938
938
939
939
940
940
941
941
942
942
943
943
944
944
945
945
946
946
947
947
948
948
949
949
950
950
951
951
952
952
953
953
954
954
955
955
956
956
957
957
958
958
959
959
960
960
961
961
962
962
963
963
964
964
965
965
966
966
967
967
968
968
969
969
970
970
971
971
972
972
973
973
974
974
975
975
976
976
977
977
978
978
979
979
980
980
981
981
982
982
983
983
984
984
985
985
986
986
987
987
988
988
989
989
990
990
991
991
992
992
993
993
994
994
995
995
996
996
997
997
998
998
999
999
1000
1000
1001
1001
1002
1002
1003
1003
1004
1004
1005
1005
1006
1006
1007
1007
1008
1008
1009
1009
1010
1010
1011
1011
1012
1012
1013
1013
1014
1014
1015
1015
1016
1016
1017
1017
1018
1018
1019
1019
1020
1020
1021
1021
1022
1022
1023
1023
1024
1024
1025
1025
1026
1026
1027
1027
1028
1028
1029
1029
1030
1030
1031
1031
1032
1032
1033
1033
1034
1034
1035
1035
1036
1036
1037
1037
1038
1038
1039
1039
1040
1040
1041
1041
1042
1042
1043
1043
1044
1044
1045
1045
1046
1046
1047
1047
1048
1048
1049
1049
1050
1050
1051
1051
1052
1052
1053
1053
1054
1054
1055
1055
1056
1056
1057
1057
1058
1058
1059
1059
1060
1060
1061
1061
1062
1062
1063
1063
1064
1064
1065
1065
1066
1066
1067
1067
1068
1068
1069
1069
1070
1070
1071
1071
1072
1072
1073
1073
1074
1074
1075
1075
1076
1076
1077
1077
1078
1078
1079
1079
1080
1080
1081
1081
1082
1082
1083
1083
1084
1084
1085
1085
1086
1086
1087
1087
1088
1088
1089
1089
1090
1090
1091
1091
1092
1092
1093
1093
1094
1094
1095
1095
1096
1096
1097
1097
1098
1098
1099
1099
1100
1100
1101
1101
1102
1102
1103
1103
1104
1104
1105
1105
1106
1106
1107
1107
1108
1108
1109
1109
1110
1110
1111
1111
1112
1112
1113
1113
1114
1114
1115
1115
1116
1116
1117
1117
1118
1118
1119
1119
1120
1120
1121
1121
1122
1122
1123
1123
1124
1124
1125
1125
1126
1126
1127
1127
1128
1128
1129
1129
1130
1130
1131
1131
1132
1132
1133
1133
1134
1134
1135
1135
1136
1136
1137
1137
1138
1138
1139
1139
1140
1140
1141
1141
1142
1142
1143
1143
1144
1144
1145
1145
1146
1146
1147
1147
1148
1148
1149
1149
1150
1150
1151
1151
1152
1152
1153
1153
1154
1154
1155
1155
1156
1156
1157
1157
1158
1158
1159
1159
1160
1160
1161
1161
1162
1162
1163
1163
1164
1164
1165
1165
1166
1166
1167
1167
1168
1168
1169
1169
1170
1170
1171
1171
1172
1172
1173
1173
1174
1174
1175
1175
1176
1176
1177
1177
1178
1178
1179
1179
1180
1180
1181
1181
1182
1182
1183
1183
1184
1184
1185
1185
1186
1186
1187
1187
1188
1188
1189
1189
1190
1190
1191
1191
1192
1192
1193
1193
1194
1194
1195
1195
1196
1196
1197
1197
1198
1198
1199
1199
1200
1200
1201
1201
1202
1202
1203
1203
1204
1204
1205
1205
1206
1206
1207
1207
1208
1208
1209
1209
1210
1210
1211
1211
1212
1212
1213
1213
1214
1214
1215
1215
1216
1216
1217
1217
1218
1218
1219
1219
1220
1220
1221
1221
1222
1222
1223
1223
1224
1224
1225
1225
1226
1226
1227
1227
1228
1228
1229
1229
1230
1230
1231
1231
1232
1232
1233
1233
1234
1234
1235
1235
1236
1236
1237
1237
1238
1238
1239
1239
1240
1240
1241
1241
1242
1242
1243
1243
1244
1244
1245
1245
1246
1246
1247
1247
1248
1248
1249
1249
1250
1250
1251
1251
1252
1252
1253
1253
1254
1254
1255
1255
1256
1256
1257
1257
1258
1258
1259
1259
1260
1260
1261
1261
1262
1262
1263
1263
1264
1264
1265
1265
1266
1266
1267
1267
1268
1268
1269
1269
1270
1270
1271
1271
1272
1272
1273
1273
1274
1274
1275
1275
1276
1276
1277
1277
1278
1278
1279
1279
1280
1280
1281
1281
1282
1282
1283
1283
1284
1284
1285
1285
1286
1286
1287
1287
1288
1288
1289
1289
1290
1290
1291
1291
1292
1292
1293
1293
1294
1294
1295
1295
1296
1296
1297
1297
1298
1298
1299
1299
1300
1300
1301
1301
1302
1302
1303
1303
1304
1304
1305
1305
1306
1306
1307
1307
1308
1308
1309
1309
1310
1310
1311
1311
1312
1312
1313
1313
1314
1314
1315
1315
1316
1316
1317
1317
1318
1318
1319
1319
1320
1320
1321
1321
1322
1322
1323
1323
1324
1324
1325
1325
1326
1326
1327
1327
1328
1328
1329
1329
1330
1330
1331
1331
1332
1332
1333
1333
1334
1334
1335
1335
1336
1336
1337
1337
1338
1338
1339
1339
1340
1340
1341
1341
1342
1342
1343
1343
1344
1344
1345
1345
1346
1346
1347
1347
1348
1348
1349
1349
1350
1350
1351
1351
1352
1352
1353
1353
1354
1354
1355
1355
1356
1356
1357
1357
1358
1358
1359
1359
1360
1360
1361
1361
1362
1362
1363
1363
1364
1364
1365
1365
1366
1366
1367
1367
1368
1368
1369
1369
1370
1370
1371
1371
1372
1372
1373
1373
1374
1374
1375
1375
1376
1376
1377
1377
1378
1378
1379
1379
1380
1380
1381
1381
1382
1382
1383
1383
1384
1384
1385
1385
1386
1386
1387
1387
1388
1388
1389
1389
1390
1390
1391
1391
1392
1392
1393
1393
1394
1394
1395
1395
1396
1396
1397
1397
1398
1398
1399
1399
1400
1400
1401
1401
1402
1402
1403
1403
1404
1404
1405
1405
1406
1406
1407
1407
1408
1408
1409
1409
1410
1410
1411
1411
1412
1412
1413
1413
1414
1414
1415
1415
1416
1416
1417
1417
1418
1418
1419
1419
1420
1420
1421
1421
1422
1422
1423
1423
1424
1424
1425
1425
1426
1426
1427
1427
1428
1428
1429
1429
1430
1430
1431
1431
1432
1432
1433
1433
1434
1434
1435
1435
1436
1436
1437
1437
1438
1438
1439
1439
1440
1440
1441
1441
1442
1442
1443
1443
1444
1444
1445
1445
1446
1446
1447
1447
1448
1448
1449
1449
1450
1450
1451
1451
1452
1452
1453
1453
1454
1454
1455
1455
1456
1456
1457
1457
1458
1458
1459
1459
1460
1460
1461
1461
1462
1462
1463
1463
1464
1464
1465
1465
1466
1466
1467
1467
1468
1468
1469
1469
1470
1470
1471
1471
1472
1472
1473
1473
1474
1474
1475
1475
1476
1476
1477
1477
1478
1478
1479
1479
1480
1480
1481
1481
1482
1482
1483
1483
1484
1484
1485
1485
1486
1486
1487
1487
1488
1488
1489
1489
1490
1490
1491
1491
1492
1492
1493
1493
1494
1494
1495
1495
1496
1496
1497
1497
1498
1498
1499
1499
1500
1500
1501
1501
1502
1502
1503
1503
1504
1504
1505
1505
1506
1506
1507
1507
1508
1508
1509
1509
1510
1510
1511
1511
1512
1512
1513
1513
1514
1514
1515
1515
1516
1516
1517
1517
1518
1518
1519
1519
1520
1520
1521
1521
1522
1522
1523
1523
1524
1524
1525
1525
1526
1526
1527
1527
1528
1528
1529
1529
1530
1530
1531
1531
1532
1532
1533
1533
1534
1534
1535
1535
1536
1536
1537
1537
1538
1538
1539
1539
1540
1540
1541
1541
1542
1542
1543
1543
1544
1544
1545
1545
1546
1546
1547
1547
1548
1548
1549
1549
1550
1550
1551
1551
1552
1552
1553
1553
1554
1554
1555
1555
1556
1556
1557
1557
1558
1558
1559
1559
1560
1560
1561
1561
1562
1562
1563
1563
1564
1564
1565
1565
1566
1566
1567
1567
```

```

33     sampled_tokens = torch.gather(batched_indices, -1, sampled_idx).
34     squeeze(-1)
35     sampled_tokens[..., 0] = cls_token_id
36
37     # Reconstruct full sequence
38     z_expanded = z.unsqueeze(1).repeat(1, n, 1)[..., c:]
39     return torch.cat((sampled_tokens, z_expanded), dim=-1)
40
41 from torch import nn
42 def OneShotCD(tfe: nn.Module, tfy: nn.Module, batch: dict[str, torch.
43     Tensor], c: int, n: int, eps: float=1e-6, topk: int=20, k: int
44     =2.75, p=0.8) -> torch.Tensor:
45     """ tfe, tfy: are the two autoregressive transformers (event type
46     and label)
47     batch: dictionary containing a batch of input_ids and
48     attention_mask of shape (bs, L) to explain.
49     c: scalar number defining the minimum context to start
50     inferring, also the sampling interval.
51     n: scalar number representing the number of samples for the
52     sampling method.
53     eps: float for numerical stability
54     topk: The number of top-k most probable tokens to keep for
55     sampling
56     k: Number of standard deviations to add to the mean for
57     dynamic threshold calculation
58     p: Probability mass for top-p nucleus
59     """
60
61     o = tfe(attention_mask=batch['attention_mask'], input_ids=batch['
62     input_ids'])['prediction_logits'] # Infer the next event type
63     x_hat = torch.nn.functional.softmax(o, dim=-1)
64
65     b_sampled = topk_p_sampling(batch['input_ids'], x_hat, c, k=topk,
66     n=n, p=p) # Sampling up to (bs, n, L)
67     n_att_mask = batch['attention_mask'].unsqueeze(1).repeat(1, n, 1)
68
69     with torch.inference_mode():
70         o = tfy(attention_mask=n_att_mask.reshape(-1, b_sampled.size
71         (-1)), input_ids=b_sampled.reshape(-1, b_sampled.size(-1))) # #
72         flatten and infer
73         prob_y_sampled = o['ep_prediction'].reshape(b_sampled.size(0),
74         n, batch['input_ids'].size(-1)-c, -1) # reshape to (bs, n, L-c)
75
76         # Ensure probs are within (eps, 1-eps)
77         prob_y_sampled = torch.clamp(prob_y_sampled, eps, 1 - eps)
78
79         y_hat_i = prob_y_sampled[..., :-1, :] # P(Yj|z)
80         y_hat_iplus1 = prob_y_sampled[..., 1:, :] # P(Yj|z, x_i)
81
82         # Compute the CMI & CS and average across sampling dim
83         cmi = torch.mean(y_hat_iplus1*torch.log(y_hat_iplus1/y_hat_i)+
84         (1-y_hat_iplus1)*torch.log((1-y_hat_iplus1)/(1-y_hat_i)), dim=1)
85         # (BS, L, Y)
86         cs = y_hat_iplus1 - y_hat_i
87         cs_mean = torch.mean(cs, dim=1)
88         cs_std = torch.std(cs, dim=1)
89
90         # Confidence interval for threshold
91         mu = cmi.mean(dim=1)
92         std = cmi.std(dim=1)
93         dynamic_thresholds = mu + std * k
94
95         # Broadcast to select an individual dynamic threshold
96         cmi_mask = cmi >= dynamic_thresholds.unsqueeze(1)
97
98         cause_token_indices = cmi_mask.nonzero(as_tuple=False)
99
100
101
102
103
104
105
106
107
108
109
110
111
112
113
114
115
116
117
118
119
120
121
122
123
124
125
126
127
128
129
130
131
132
133
134
135
136
137
138
139
140
141
142
143
144
145
146
147
148
149
150
151
152
153
154
155
156
157
158
159
160
161
162
163
164
165
166
167
168
169
170
171
172
173
174
175
176
177
178
179
180
181
182
183
184
185
186
187
188
189
190
191
192
193
194
195
196
197
198
199
200
201
202
203
204
205
206
207
208
209
210
211
212
213
214
215
216
217
218
219
220
221
222
223
224
225
226
227
228
229
230
231
232
233
234
235
236
237
238
239
240
241
242
243
244
245
246
247
248
249
250
251
252
253
254
255
256
257
258
259
260
261
262
263
264
265
266
267
268
269
270
271
272
273
274
275
276
277
278
279
280
281
282
283
284
285
286
287
288
289
290
291
292
293
294
295
296
297
298
299
300
301
302
303
304
305
306
307
308
309
310
311
312
313
314
315
316
317
318
319
320
321
322
323
324
325
326
327
328
329
330
331
332
333
334
335
336
337
338
339
340
341
342
343
344
345
346
347
348
349
350
351
352
353
354
355
356
357
358
359
360
361
362
363
364
365
366
367
368
369
370
371
372
373
374
375
376
377
378
379
380
381
382
383
384
385
386
387
388
389
390
391
392
393
394
395
396
397
398
399
400
401
402
403
404
405
406
407
408
409
410
411
412
413
414
415
416
417
418
419
420
421
422
423
424
425
426
427
428
429
430
431
432
433
434
435
436
437
438
439
440
441
442
443
444
445
446
447
448
449
450
451
452
453
454
455
456
457
458
459
460
461
462
463
464
465
466
467
468
469
470
471
472
473
474
475
476
477
478
479
480
481
482
483
484
485
486
487
488
489
490
491
492
493
494
495
496
497
498
499
500
501
502
503
504
505
506
507
508
509
510
511
512
513
514
515
516
517
518
519
520
521
522
523
524
525
526
527
528
529
530
531
532
533
534
535
536
537
538
539
540
541
542
543
544
545
546
547
548
549
550
551
552
553
554
555
556
557
558
559
560
561
562
563
564
565
566
567
568
569
570
571
572
573
574
575
576
577
578
579
580
581
582
583
584
585
586
587
588
589
589
590
591
592
593
594
595
596
597
598
599
600
601
602
603
604
605
606
607
608
609
610
611
612
613
614
615
616
617
618
619
620
621
622
623
624
625
626
627
628
629
630
631
632
633
634
635
636
637
638
639
640
641
642
643
644
645
646
647
648
649
649
650
651
652
653
654
655
656
657
658
659
659
660
661
662
663
664
665
666
667
668
669
669
670
671
672
673
674
675
676
677
678
679
679
680
681
682
683
684
685
686
687
687
688
689
689
690
691
692
693
694
695
696
697
697
698
699
699
700
701
702
703
704
705
706
707
708
709
709
710
711
712
713
714
715
716
717
718
719
719
720
721
722
723
724
725
726
727
727
728
729
729
730
731
732
733
734
735
735
736
737
737
738
739
739
740
741
742
743
744
745
745
746
747
747
748
749
749
750
751
752
753
753
754
755
755
756
757
757
758
759
759
760
761
761
762
763
763
764
765
765
766
767
767
768
768
769
769
770
771
771
772
773
773
774
775
775
776
777
777
778
779
779
780
781
781
782
783
783
784
785
785
786
787
787
788
789
789
790
791
791
792
793
793
794
795
795
796
797
797
798
799
799
800
801
801
802
803
803
804
805
805
806
807
807
808
809
809
810
811
811
812
813
813
814
815
815
816
817
817
818
819
819
820
821
821
822
823
823
824
825
825
826
827
827
828
829
829
830
831
831
832
833
833
834
835
835
836
837
837
838
839
839
840
841
841
842
843
843
844
845
845
846
847
847
848
849
849
850
851
851
852
853
853
854
855
855
856
857
857
858
859
859
860
861
861
862
863
863
864
865
865
866
867
867
868
869
869
870
871
871
872
873
873
874
875
875
876
877
877
878
879
879
880
881
881
882
883
883
884
885
885
886
887
887
888
889
889
890
891
891
892
893
893
894
895
895
896
897
897
898
899
899
900
901
901
902
903
903
904
905
905
906
907
907
908
909
909
910
911
911
912
913
913
914
915
915
916
917
917
918
919
919
920
921
921
922
923
923
924
925
925
926
927
927
928
929
929
930
931
931
932
933
933
934
935
935
936
937
937
938
939
939
940
941
941
942
943
943
944
945
945
946
947
947
948
949
949
950
951
951
952
953
953
954
955
955
956
957
957
958
959
959
960
961
961
962
963
963
964
965
965
966
967
967
968
969
969
970
971
971
972
973
973
974
975
975
976
977
977
978
979
979
980
981
981
982
983
983
984
985
985
986
987
987
988
989
989
990
991
991
992
993
993
994
995
995
996
997
997
998
999
999
1000
1000
1001
1001
1002
1002
1003
1003
1004
1004
1005
1005
1006
1006
1007
1007
1008
1008
1009
1009
1010
1010
1011
1011
1012
1012
1013
1013
1014
1014
1015
1015
1016
1016
1017
1017
1018
1018
1019
1019
1020
1020
1021
1021
1022
1022
1023
1023
1024
1024
1025
1025
1026
1026
1027
1027
1028
1028
1029
1029
1030
1030
1031
1031
1032
1032
1033
1033
1034
1034
1035
1035
1036
1036
1037
1037
1038
1038
1039
1039
1040
1040
1041
1041
1042
1042
1043
1043
1044
1044
1045
1045
1046
1046
1047
1047
1048
1048
1049
1049
1050
1050
1051
1051
1052
1052
1053
1053
1054
1054
1055
1055
1056
1056
1057
1057
1058
1058
1059
1059
1060
1060
1061
1061
1062
1062
1063
1063
1064
1064
1065
1065
1066
1066
1067
1067
1068
1068
1069
1069
1070
1070
1071
1071
1072
1072
1073
1073
1074
1074
1075
1075
1076
1076
1077
1077
1078
1078
1079
1079
1080
1080
1081
1081
1082
1082
1083
1083
1084
1084
1085
1085
1086
1086
1087
1087
1088
1088
1089
1089
1090
1090
1091
1091
1092
1092
1093
1093
1094
1094
1095
1095
1096
1096
1097
1097
1098
1098
1099
1099
1100
1100
1101
1101
1102
1102
1103
1103
1104
1104
1105
1105
1106
1106
1107
1107
1108
1108
1109
1109
1110
1110
1111
1111
1112
1112
1113
1113
1114
1114
1115
1115
1116
1116
1117
1117
1118
1118
1119
1119
1120
1120
1121
1121
1122
1122
1123
1123
1124
1124
1125
1125
1126
1126
1127
1127
1128
1128
1129
1129
1130
1130
1131
1131
1132
1132
1133
1133
1134
1134
1135
1135
1136
1136
1137
1137
1138
1138
1139
1139
1140
1140
1141
1141
1142
1142
1143
1143
1144
1144
1145
1145
1146
1146
1147
1147
1148
1148
1149
1149
1150
1150
1151
1151
1152
1152
1153
1153
1154
1154
1155
1155
1156
1156
1157
1157
1158
1158
1159
1159
1160
1160
1161
1161
1162
1162
1163
1163
1164
1164
1165
1165
1166
1166
1167
1167
1168
1168
1169
1169
1170
1170
1171
1171
1172
1172
1173
1173
1174
1174
1175
1175
1176
1176
1177
1177
1178
1178
1179
1179
1180
1180
1181
1181
1182
1182
1183
1183
1184
1184
1185
1185
1186
1186
1187
1187
1188
1188
1189
1189
1190
1190
1191
1191
1192
1192
1193
1193
1194
1194
1195
1195
1196
1196
1197
1197
1198
1198
1199
1199
1200
1200
1201
1201
1202
1202
1203
1203
1204
1204
1205
1205
1206
1206
1207
1207
1208
1208
1209
1209
1210
1210
1211
1211
1212
1212
1213
1213
1214
1214
1215
1215
1216
1216
1217
1217
1218
1218
1219
1219
1220
1220
1221
1221
1222
1222
1223
1223
1224
1224
1225
1225
1226
1226
1227
1227
1228
1228
1229
1229
1230
1230
1231
1231
1232
1232
1233
1233
1234
1234
1235
1235
1236
1236
1237
1237
1238
1238
1239
1239
1240
1240
1241
1241
1242
1242
1243
1243
1244
1244
1245
1245
1246
1246
1247
1247
1248
1248
1249
1249
1250
1250
1251
1251
1252
1252
1253
1253
1254
1254
1255
1255
1256
1256
1257
1257
1258
1258
1259
1259
1260
1260
1261
1261
1262
1262
1263
1263
1264
1264
1265
1265
1266
1266
1267
1267
1268
1268
1269
1269
1270
1270
1271
1271
1272
1272
1273
1273
1274
1274
1275
1275
1276
1276
1277
1277
1278
1278
1279
1279
1280
1280
1281
1281
1282
1282
1283
1283
1284
1284
1285
1285
1286
1286
1287
1287
1288
1288
1289
1289
1290
1290
1291
1291
1292
1292
1293
1293
1294
1294
1295
1295
1296
1296
1297
1297
1298
1298
1299
1299
1300
1300
1301
1301
1302
1302
1303
1303
1304
1304
1305
1305
1306
1306
1307
1307
1308
1308
1309
1309
1310
1310
1311
1311
1312
1312
1313
1313
1314
1314
1315
1315
1316
1316
1317
1317
1318
1318
1319
1319
1320
1320
1321
1321
1322
1322
1323
1323
1324
1324
1325
1325
1326
1326
1327
1327
1328
1328
1329
1329
1330
1330
1331
1331
1332
1332
1333
1333
1334
1334
1335
1335
1336
1336
1337
1337
1338
1338
1339
1339
1340
1340
1341
1341
1342
1342
1343
1343
1344
1344
1345
1345
1346
1346
1347
1347
1348
1348
1349
1349
1350
1350
1351
1351
1352
1352
1353
1353
1354
1354
1355
1355
1356
1356
1357
1357
1358
1358
1359
1359
1360
1360
1361
1361
1362
1362
1363
1363
1364
1364
1365
1365
1366
1366
1367
1367
1368
1368
1369
1369
1370
1370
1371
1371
1372
1372
1373
1373
1374
1374
1375
1375
1376
1376
1377
1377
1378
1378
1379
1379
1380
1380
1381
1381
1382
1382
1383
1383
1384
1384
1385
1385
1386
1386
1387
1387
1388
1388
1389
1389
1390
1390
1391
1391
1392
1392
1393
1393
1394
1394
1395
1395
1396
1396
1397
1397
1398
1398
1399
1399
1400
1400
1401
1401
1402
1402
1403
1403
1404
1404
1405
1405
1406
1406
1407
1407
1408
1408
1409
1409
1410
1410
1411
1411
1412
1412
1413
1413
1414
1414
1415
1415
1416
1416
1417
1417
1418
1418
1419
1419
1420
1420
1421
1421
1422
1422
1423
1423
1424
1424
1425
1425
1426
1426
1427
1427
1428
1428
1429
1429
1430
1430
1431
1431
1432
1432
1433
1433
1434
1434
1435
1435
1436
1436
1437
1437
1438
1438
1439
1439
1440
1440
1441
1441
1442
1442
1443
1443
1444
1444
1445
1445
1446
1446
1447
1447
1448
1448
1449
1449
1450
1450
1451
1451
1452
1452
1453
1453
1454
1454
1455
1455
1456
1456
1457
1457
1458
1458
1459
1459
1460
1460
1461
1461
1462
1462
1463
1463
1464
1464
1465
1465
1466
1466
1467
1467
1468
1468
1469
1469
1470
1470
1471
1471
1472
1472
1473
1473
1474
1474
1475
1475
1476
1476
1477
1477
1478
1478
1479
1479
1480
1480
1481
1481
1482
1482
1483
1483
1484
1484
1485
1485
1486
1486
1487
1487
1488
1488
1489
1489
1490
1490
1491
1491
1492
1492
1493
1493
1494
1494
1495
1495
1496
1496
1497
1497
1498
1498
1499
1499
1500
1500
1501
1501
1502
1502
1503
1503
1504
1504
1505
1505
1506
1506
1507
1507
1508
1508
1509
1509
1510
1510
1511
1511
1512
1512
1513
1513
1514
1514
1515
1515
1516
1516
1517
1517
1518
1518
1519
1519
1520
1520
1521
1521
1522
1522
1523
1523
1524
1524
1525
1525
1526
1526
1527
1527
1528
1528
1529
1529
1530
1530
1531
1531
1532
1532
1533
1533
1534
1534
1535
1535
1536
1536
1537
1537
1538
1538
1539
1539
1540
1540
1541
1541
1542
1542
1543
1543
1544
1544
1545
1545
1546
1546
1547
1547
1548
1548
1549
1549
1550
1550
1551
1551
1552
1552
1553
1553
1554
1554
1555
1555
1556
1556
1557
1557
1558
1558
1559
1559
1560
1560
1561
1561
1562
1562
1563
1563
1564
1564
1565
1565
1566
1566
1567
1567
1568
1568
1569
1569
1570
1570
1571
1571
1572
1572
1573
1573
1574
1574
1575
1575
1576
1576
1577
1577
1578
1578
1579
1579
1580
1580
1581
1581
1582
1582
1583
1583
1584
1584
1585
1585
1586
1586
1587
1587
1588
1588
1589
1589
1590
1590
1591
1591
1592
1592
1593
1593
1594
1594
1595
1595
1596
1596
1597
1597
1598
1598
1599
1599
1600
1600
1601
1601
1602
1602
1603
1603
1604
1604
1605
1605
1606
1606
1607
1607
1608
1608
1609
1609
1610
1610
1611
1611
1612
1612
1613
1613
1614
1614
1615
1615
1616
1616
1617
1617
1618
1618
1619
1619
1620
1620
1621
1621
1622
1622
1623
1623
1624
1624
1625
1625
1626
1626
1627
1627
1628
1628
1629
1629
1630
1630
1631
1631
1632
1632
1633
1633
1634
1634
1635
1635
1636
1636
1637
1637
1638
1638
1639
1639
1640
1640
1641
1641
1642
1642
1643
1643
1644
1644
1645
1645
1646
1646
1647
1647
1648
1648
1649
1649
1650
1650
1651
1651
1652
1652
1653
1653
1654
1654
1655
1655
1656
1656
1657
1657
1658
1658
1659
1659
1660
1660
1661
1661
1662
1662
1663
1663
1664
1664
1665
1665
1666
1666
1667
1667
1668
1668
1669
1669
1670
1670
1671
1671
1672
1672
1673
1673
1674
1674
1675
1675
1676
1676
1677
1677
1678
1678
1679
1679
1680
1680
1681
1681
1682
1682
1683
1683
1684
1684
1685
1685
1686
1686
1687
1687
1688
1688
1689
1689
1690
1690
1691
1691
1692
1692
1693
1693
1694
1694
1695
1695
1696
1696
1697
1697
1698
1698
1699
1699
1700
1700
1701
1701
1702
1702
1703
1703
1704
1704
1705
1705
1706
1706
1707
1707
1708
1708
1709
1709
1710
1710
1711
1711
1712
1712
1713
1713
1714
1714
1715
1715
1716
1716
1717
1717
1718
1718
1719
1719
1720
1720
1721
1721
1722
1722
1723
1723
```

```
83         # (num_causes, 3) --> each row is [batch_idx, position_idx, label_idx]
84     return cause_token_indices, cs_mean, cs_std, cmi_mask
```

Remark. Since `tfy` contains `tfe` as backbone, in practice we need only one forward pass from `tfy` and extract also \hat{x} , so `tfe` is not needed. We let it to improve understanding and clarity.

D.3 Phase 2.

```

49     edge_counts = defaultdict(lambda: defaultdict(int)) # edge_counts
50     [label][token] = count
51
52     for g in graphs:
53         for label, token_dict in g.items():
54             if label not in labels:
55                 continue
56             for token in token_dict:
57                 edge_counts[label][token] += 1
58
59     # Step 3: Keep edges above frequency threshold
60     filtered_labels = defaultdict(dict)
61     for label in labels:
62         total = sample_per_label.get(label, samples) # fallback to
63         total_graphs if missing
64         for token, count in edge_counts[label].items():
65             freq = count / total
66             if freq >= auto_threshold_fn(sample_per_label.get(label,
67                 1)):
68                 filtered_labels[label][token] = {'frequency': freq}
69             if verbose:
70                 print(f"[{label}] token {token} kept (freq={freq
71                 :.2f})")
72
73     nb_of_edges = sum(len(v) for v in filtered_labels.values())
74     print(f"Time: {(datetime.now() - start_time).total_seconds():.2f}s")
75
76     return filtered_labels, sample_per_label, (datetime.now() -
77         start_time).total_seconds()

```

E Figures

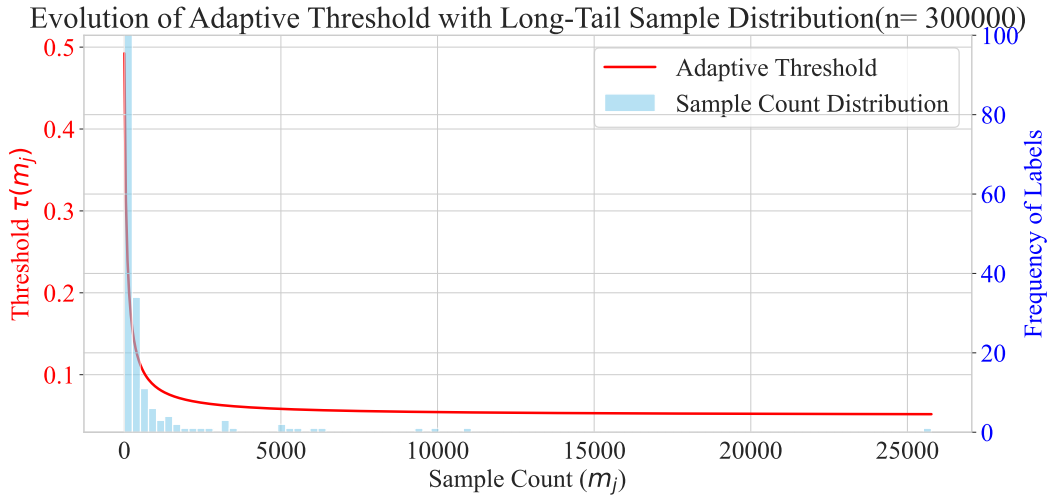


Figure 7: Adaptive thresholding function $\tau_j(m_j)$ across varying label frequencies m_j , illustrating the logistic decay from τ_{\max} to τ_{\min} .

Figure 8: Illustration of structural fusion: individual causal graphs (left) aggregated into a fused DAG for multi-label event sequences (right) using a simple union.

